OPEN ACCESS Freely available online

PLoS GENETICS

# Diverse Roles and Interactions of the SWI/SNF Chromatin Remodeling Complex Revealed Using Global Approaches

**Ghia M. Euskirchen[1☯], Raymond K. Auerbach[2☯], Eugene Davidov[3], Tara A. Gianoulis[4], Guoneng Zhong[5], Joel Rozowsky[2,6], Nitin Bhardwaj[2], Mark B. Gerstein[2,6], Michael Snyder[1]***

**1** Department of Genetics, Stanford University School of Medicine, Stanford, California, United States of America, **2** Program in Computational Biology and Bioinformatics, Yale University, New Haven, Connecticut, United States of America, **3** PerkinElmer, Shelton, Connecticut, United States of America, **4** Department of Genetics and Wyss Institute for Bio-Inspired Engineering, Harvard Medical School, Boston, Massachusetts, United States of America, **5** Yale Center for Medical Informatics, Yale University, New Haven, Connecticut, United States of America, **6** Department of Molecular Biophysics and Biochemistry, Yale University, New Haven, Connecticut, United States of America

## Abstract

A systems understanding of nuclear organization and events is critical for determining how cells divide, differentiate, and respond to stimuli and for identifying the causes of diseases. Chromatin remodeling complexes such as SWI/SNF have been implicated in a wide variety of cellular processes including gene expression, nuclear organization, centromere function, and chromosomal stability, and mutations in SWI/SNF components have been linked to several types of cancer. To better understand the biological processes in which chromatin remodeling proteins participate, we globally mapped binding regions for several components of the SWI/SNF complex throughout the human genome using ChIP-Seq. SWI/SNF components were found to lie near regulatory elements integral to transcription (e.g. 5′ ends, RNA Polymerases II and III, and enhancers) as well as regions critical for chromosome organization (e.g. CTCF, lamins, and DNA replication origins). Interestingly we also find that certain configurations of SWI/SNF subunits are associated with transcripts that have higher levels of expression, whereas other configurations of SWI/SNF factors are associated with transcripts that have lower levels of expression. To further elucidate the association of SWI/SNF subunits with each other as well as with other nuclear proteins, we also analyzed SWI/SNF immunoprecipitated complexes by mass spectrometry. Individual SWI/SNF factors are associated with their own family members, as well as with cellular constituents such as nuclear matrix proteins, key transcription factors, and centromere components, implying a ubiquitous role in gene regulation and nuclear function. We find an overrepresentation of both SWI/SNF-associated regions and proteins in cell cycle and chromosome organization. Taken together the results from our ChIP and immunoprecipitation experiments suggest that SWI/SNF facilitates gene regulation and genome function more broadly and through a greater diversity of interactions than previously appreciated.

**Citation:** Euskirchen GM, Auerbach RK, Davidov E, Gianoulis TA, Zhong G, et al. (2011) Diverse Roles and Interactions of the SWI/SNF Chromatin Remodeling Complex Revealed Using Global Approaches. PLoS Genet 7(3): e1002008. doi:10.1371/journal.pgen.1002008

**Editor:** Gregory P. Copenhaver, The University of North Carolina at Chapel Hill, United States of America

**Received** October 4, 2010; **Accepted** January 4, 2011; **Published** March 3, 2011



**Funding:** This work was supported by grants from the NIH. RKA was supported by a predoctoral fellowship in informatics from the National Library of Medicine. The funders had no role in study design, data collection and analysis, decision to publish, or preparation of the manuscript.

**Competing Interests:** The authors have declared that no competing interests exist.

* E-mail: mpsnyder@stanford.edu

☯ These authors contributed equally to this work.

## Introduction

Chromosomes undergo a wide variety of dynamic processes including transcription, replication, repair and packaging. Each of these activities requires the recruitment and congregation of a particular set of factors and chromosomal elements. For example visualization of nascent mRNA in HeLa cells has led to a model of transcription units being clustered into "factories" thereby facilitating optimal engagement of RNA Polymerase II (Pol II) and coordination with other crucial holoenzyme complexes [1–3]. In addition to RNA Pol II and transcription factors, transcriptional assemblages include proteins critical to regulating chromatin. The accessibility of nuclear proteins to DNA is often controlled by ATP-dependent chromatin remodeling complexes, which are thought to play a role in a number of different cellular transactions by reshaping the epigenetic landscape.

The SWI/SNF (switch/sucrose nonfermentable) chromatin remodeling proteins were first discovered in *Saccharomyces cerevisiae* as components of a 2 MDa complex that repositions nucleosomes for vital tasks such as transcriptional control, DNA repair, recombination and chromosome segregation [4,5]. Mammalian SWI/SNF is comprised of approximately ten subunits and the combinations of these subunits, some of which have multiple isoforms, enable multiple varieties of SWI/SNF complexes to exist both within a given cell and across cell types [6]. Among these subunits either of the two ATPases, Brg1 or Brm, is sufficient to remodel nucleosome arrays *in vitro*, however maximal nucleosome remodeling activity is achieved when the SWI/SNF subunits BAF155, BAF170 and Ini1 are present in a 2:1 stoichiometry relative to Brg1 [7]. Whereas the ATPases have an obvious catalytic function, the roles of the other SWI/SNF subunits are largely obscure. Several reports indicate that BAF155 and BAF170 provide scaffolding functions for other SWI/SNF subunits as well as regulating their protein levels [8,9]. SWI/SNF also contains β-actin and the actin-related protein BAF53, suggesting a possible bridge to nuclear organization or signal transduction, e.g. through phosphatidylinositol signaling [10,11]. Phosphatidylinositol 4,5-bisphosphate has been shown to bind to Brg1 and promote

## Author Summary

Genetic information and programming are not entirely contained in DNA sequence but are also governed by chromatin structure. Gaining a greater understanding of chromatin remodeling complexes can bridge gaps between processes in the genome and the epigenome and can offer insights into diseases such as cancer. We identified targets of the chromatin remodeling complex, SWI/SNF, on a genome-wide scale using ChIP-Seq. We also identify proteins that co-purify with its various components via immunoprecipitation combined with mass spectrometry. By integrating these newly-identified regions with a combination of novel and published data sources, we identify pathways and cellular compartments in which SWI/SNF plays a major role as well as discern general characteristics of SWI/SNF target sites. Our parallel evaluations of multiple SWI/SNF factors indicate that these subunits are found in highly dynamic and combinatorial assemblies. Our study presents the first genome-wide and unified view of multiple SWI/SNF components and also provides a valuable resource to the scientific community as an important data source to be integrated with future genomic and epigenomic studies.


binding to actin filaments [12]. Mutations resulting in loss of Ini1 function are associated with rare but aggressive pediatric cancers [13,14]. The SWI/SNF subunits Brg1 [15] and ARID1A [16–18] are likewise thought to have tumor suppressor roles based on mutations recovered from other tumor types. Curiously, Ini1 alone has a unique and largely undefined role in HIV-1 infection that includes binding of Ini1 to HIV-1 integrase and the cytoplasmic export of Ini1 and its incorporation into HIV-1 particles [19–21].

The role of SWI/SNF components in cancer and tumor suppression is poorly understood despite extensive study. Detailed investigations of individual loci have implicated SWI/SNF in various transcriptional pathways including the cell cycle and p53 signaling [22], insulin signaling [23], and TGFβ signaling [24], as well as signaling through several different nuclear hormone receptors [25]. Although *in vitro* experiments and single-gene studies have been informative and have laid the foundation for understanding chromatin remodeling, a global analysis of targets of SWI/SNF is expected to yield a more extensive view into the biological roles of SWI/SNF components and their involvement in human disease.

In this study we present two complementary global analyses of SWI/SNF subunits to provide a more systematic view of SWI/SNF functions. First we performed ChIP-Seq with the ubiquitous SWI/SNF components Ini1, BAF155, BAF170 as well as the Brg1 ATPase. Second, in a parallel set of studies we performed mass spectrometry identification of proteins that co-immunoprecipitate with SWI/SNF components. Using our ChIP-Seq results the resulting chromosomal locations were integrated with published annotations to yield a more complete understanding of SWI/SNF on a genome-wide scale. We find SWI/SNF components frequently occupy transcription start sites (TSSs), enhancers, CTCF regions and many regions occupied by Pol II. Further analyses of the SWI/SNF regions we identified by ChIP-Seq reveals that SWI/SNF factors target genes and signaling pathways involved in cell proliferation and cancer. Our investigation of SWI/SNF protein interactions detected not only the expected co-occurrences of individual SWI/SNF factors with each other but also with cellular components such as nuclear matrix proteins, key transcription factors and centromere proteins implying a ubiquitous role in gene regulation and nuclear function. We find an overrepresentation of both SWI/SNF-associated chromosomal regions and proteins in cell cycle and chromosome organization. Collectively our results suggest that SWI/SNF is at the nexus of multiple signal transduction pathways, essential chromosomal functions and nuclear organization.

## Results

### Genome-wide mapping of SWI/SNF subunits reveals many different co-associations

We identified the targets of four SWI/SNF components, Ini1 (SMARCB1), Brg1 (SMARCA4), BAF155 (SMARCC1) and BAF170 (SMARCC2), using ChIP-Seq. Chromatin complexes were isolated from HeLa S3 nuclei following independent immunoprecipitations with antibodies for each factor. Each of these antibodies was characterized by both immunoblot and mass spectrometry analyses (see Materials and Methods). Reads that mapped uniquely to the genome were retained (29–33 million reads per data set; Table1) and significant binding regions were identified using the PeakSeq program with q-value$<$0.05 [26]. The peaks were compared to a similarly-sized data set of uniquely mapped ChIP DNA reads obtained from control immunoprecipitation experiments using normal IgG (i.e. a control serum that is not directed to any known antigens). Using this approach we identified many Ini1-, Brg1-, BAF155- and BAF170-associated regions (Table1).

The majority of SWI/SNF binding occurs near (±2.5 kb) protein-coding genes, a distribution that is significant relative to a random target list ($p<1\times10^{-16}$; Genome Structure Correction (GSC) test [27]; see Materials and Methods). Several examples of SWI/SNF positioning relative to genic regions are shown in Figure1 and Figure S1. In order to further examine SWI/SNF locations with respect to gene-rich and gene-poor regions we obtained a set of histone H3K27me3 domains that were identified in HeLa cells (Table S1; [28]) because this chromatin mark often occurs in gene-poor and repressed (i.e. heterochromatin) regions. Although most SWI/SNF-binding occurs outside H3K27me3 domains, we observed that SWI/SNF is occasionally found in heterochromatin regions, as shown in Figure2. In this example a 7.5 Mb heterochromatin region on Chr16 contains a single gene, the neuronal cadherin *CDH8*, that is repressed and lacks RNA Pol II, however several SWI/SNF binding regions are found nearby.

We have performed considerable analyses of the targets for the individual SWI/SNF factors, particularly with respect to elements representing several major classes of genomic features including promoters (Ensembl protein-coding genes), RNA Pol II sites [26], CTCF sites [28], and predicted enhancers [29]. All of these features were identified in HeLa cells (Table1, Tables S1 and S2; see Materials and Methods). In comparisons between the individual target lists for Ini1, Brg1, BAF155 and BAF170 with promoters, RNA Pol II sites, CTCF sites and enhancers we found that each SWI/SNF factor is significantly overrepresented for each of these major classes of genomic elements ($p<1\times10^{-16}$, GSC test, see Materials and Methods). To arrive at a single unified and more conservative list of SWI/SNF locations, we first took the union of all regions for Ini1, BAF155, BAF170 and Brg1, resulting in 69,658 SWI/SNF regions. We then trimmed this list to a high-confidence set of 49,555 sites by eliminating those regions where either only a single SWI/SNF subunit was present or that those regions that did not co-occur with either promoters, RNA Pol II sites, CTCF sites or predicted enhancers. We used this list of 49,555 SWI/SNF regions for all subsequent analyses unless otherwise noted (Table S3). The four major classes of genomic

**Table 1.** Read counts and target regions identified by ChIP-Seq.

| Data set | Number of uniquely mapped reads | Total number of targets (PeakSeq)[1] | Number of genic targets[2] | Number of targets after filtering (high-confidence union)[3] |
|---|---|---|---|---|
| Ini1 | 33,360,976 | 49,458 | 32,725 (66%) | 24,478 (49%) |
| Brg1 | 30,037,219 | 12,725 | 7,823 (61%) | 12,317 (25%) |
| BAF155 | 28,800,740 | 46,412 | 28,221 (61%) | 37,921 (77%) |
| BAF170 | 29,090,374 | 30,136 | 18,847 (63%) | 25,433 (51%) |
| Pol II | 29,060,928 | 23,320 | 18,305 (78%) | 19,669 (40%) |
| IgG control | 28,960,961 | N/A | N/A | N/A |

1 Uniquely mapped targets were identified by PeakSeq and further filtered using criteria more stringent than the default parameters. See Materials and Methods.
2 Genic regions were identified for the total number of targets determined by PeakSeq. Genic regions are defined as a window encompassing 2.5 kb up- and downstream of the 5′ and 3′ ends, respectively, using protein-coding genes from Ensembl build 52 based on hg18.
3 The high-confidence union list contains 49,555 targets and was formed by creating a union list of all SWI/SNF regions from those identified by PeakSeq and trimming this list to those SWI/SNF regions that co-occur with each other, Pol II regions, 5′ ends of protein-coding genes, CTCF sites or putative enhancers. For further details, see Materials and Methods.
doi:10.1371/journal.pgen.1002008.t001

features mentioned above were overrepresented in both the 69,658 SWI/SNF regions as well as the more conservative list 49,555 SWI/SNF regions ($p<1\times10^{-16}$, GSC test).

We next examined the configurations of our 49,555 SWI/SNF regions (Figure3A and Table2). Ini1, BAF155 and BAF170 have been described as forming a 'core' based on their ability to stimulate remodeling activity of the Brg1 ATPase in reconstitution experiments [7]. Among our data 30,310 regions (61%) have two or more SWI/SNF components and 9,760 regions (20%) contain the core of Ini1, BAF155 and BAF170; for the purposes of this study we call this the 'core set'. Among putative complexes comprised of two or more SWI/SNF subunits, we observed BAF155 was the subunit most common to each binding region. Only 770 SWI/SNF subunit co-occurrences were recovered that lacked BAF155 as compared to 6,467 for BAF170 and 14,824 for Ini1. This finding is consistent with several previous studies showing that BAF155 is important for SWI/SNF complex stability [8,9]. BAF155 may increase the stability of the complex during assembly, or BAF155 may be easier to detect by ChIP.

## Genome-wide locations of SWI/SNF components suggest diverse roles in gene regulation

One of the primary functions of chromatin remodeling complexes is to assist in gene regulation. Among the SWI/SNF regions in our high-confidence union set of 49,555 sites, 29% correspond to the 5′ ends of protein-coding Ensembl genes, 40% correspond to Pol II sites, 17% correspond to CTCF sites and 43% correspond to predicted enhancer regions (Figure3B; Table3). The various combinations of these four elements account for a total of 90% of the SWI/SNF union regions; 4,800 (10%) of the SWI/SNF regions are unclassified using the above elements. Similar trends were observed for the 9,760 SWI/SNF "core" regions where Ini1, BAF155 and BAF170 all co-occur (Table3). None of these four particular SWI/SNF subunits or any combinations thereof exhibited a differential preference for one type of element (Table S4).

There are some differences between the SWI/SNF core and union regions. The SWI/SNF core regions are overrepresented for RNA Pol II ($p<9.9\times10^{-16}$; hypergeometric test) and 5′ ends ($p<6.5\times10^{-211}$; hypergeometric test) relative to all of the SWI/SNF high-confidence union regions; however the SWI/SNF high-confidence union regions are overrepresented for enhancer regions relative to the Ini1-BAF155-BAF170 core ($p<2.4\times10^{-67}$; hypergeometric test). Neither the SWI/SNF core nor the high-confidence union regions were over- or underrepresented for CTCF sites relative to each other ($p>0.05$; hypergeometric test).

Enhancers are often characterized by long-range interactions. We examined the locations of SWI/SNF binding regions in the 150 kb *CIITA* region where numerous chromosomal looping interactions have been mapped at high resolution in HeLa cells using 3C (Chromosome Conformation Capture). Brg1 has been previously mapped at several sites in this locus in these cells [30]. Superimposition of these 3C data on our SWI/SNF ChIP-Seq data (Figure4) reveals that all six of the 3C interacting regions in the *CIITA* locus (−50 kb, −16 kb, −8 kb, pIV, +40 kb and +59 kb) are bound by SWI/SNF components. Moreover certain individual SWI/SNF component binding regions that appeared initially as orphans may now be seen as part of a complete complex when joined with a distal element. For example Ini1 at pIV when joined with BAF155 and BAF170 regions at the −16 kb element forms a SWI/SNF core. Thus in the *CTIIA* locus SWI/SNF regions are often associated with 3C regions and many of the regions bound by individual factors may in fact be part of entire SWI/SNF complexes inside the nucleus.

Overall our ChIP-Seq results are summarized in Table1, Table2, Table3, and Figure3 and indicate that SWI/SNF likely contributes to gene regulation through many different avenues in light of its binding to promoters, enhancers and CTCF sites. Furthermore SWI/SNF may facilitate looping interactions among these various elements as it has been shown *in vitro* that SWI/SNF can interact simultaneously with multiple DNA sites and generate loops between them [31]. Interestingly we found a slightly higher presence of the SWI/SNF core at TSSs and with Pol II than the SWI/SNF union regions with these elements (Table3). Thus a complete core of Ini1, BAF155 and BAF170 may be required for effective promoter function whereas only a subset of these factors may be required for enhancer function. Alternatively a full SWI/SNF core may be more difficult to recover from a single enhancer element as compared to a more compact promoter region due to the enhancer's presumed interaction with many different distal elements.

## RNA polymerases are extensively colocalized with SWI/SNF

As detailed above SWI/SNF regions are enriched for Pol II. To explore the prevalence of SWI/SNF with transcriptional machin-

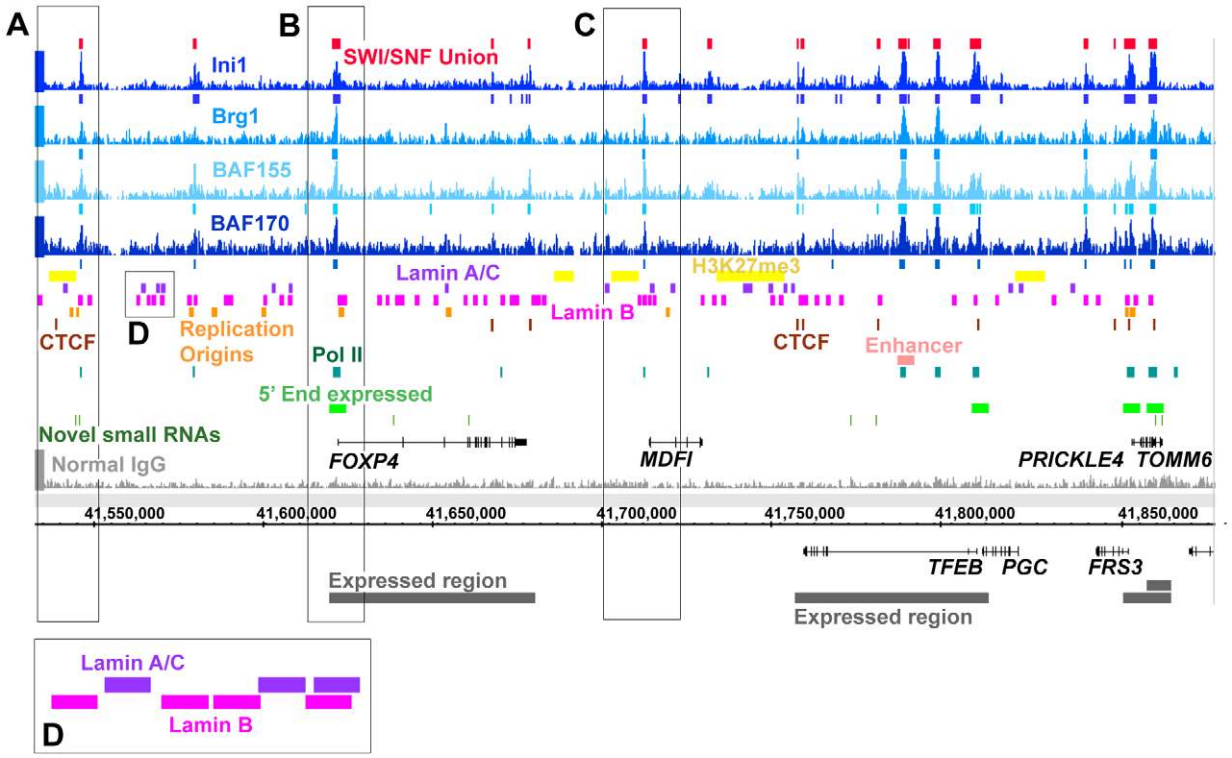
A
B
C
Ini1
SWI/SNF Union
Brg1
BAF155
BAF170
Lamin A/C
H3K27me3
Lamin B
CTCF
D
Replication Origins
Pol II
CTCF
Enhancer
5' End expressed
Novel small RNAs
Normal IgG
FOXP4
MDFI
PRICKLE4
TOMM6
41,550,000
41,600,000
41,650,000
41,700,000
41,750,000
41,800,000
41,850,000
TFEB
PGC
FRS3
Expressed region
Expressed region
Lamin A/C
Lamin B
D

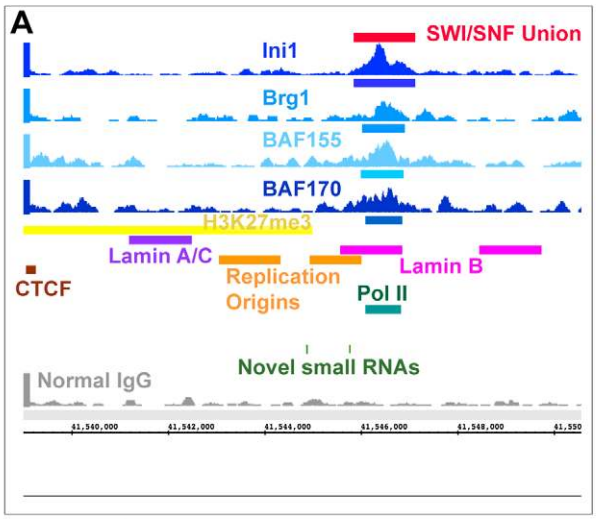
A
SWI/SNF Union
Ini1
Brg1
BAF155
BAF170
H3K27me3
Lamin A/C
Lamin B
CTCF
Replication Origins
Pol II
Novel small RNAs
Normal IgG

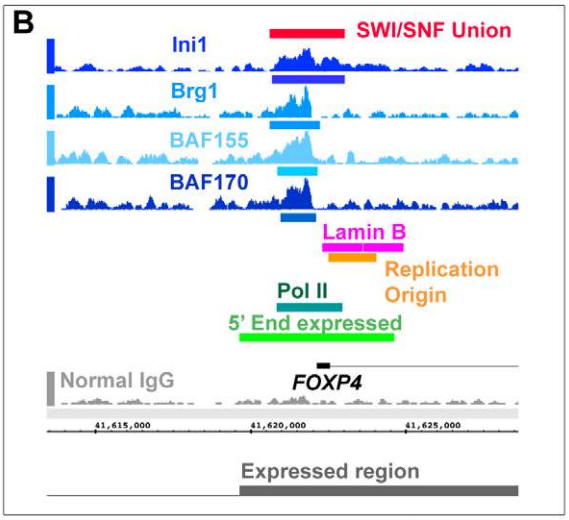
B
SWI/SNF Union
Ini1
Brg1
BAF155
BAF170
Lamin B
Replication Origin
Pol II
5' End expressed
Normal IgG
FOXP4
Expressed region

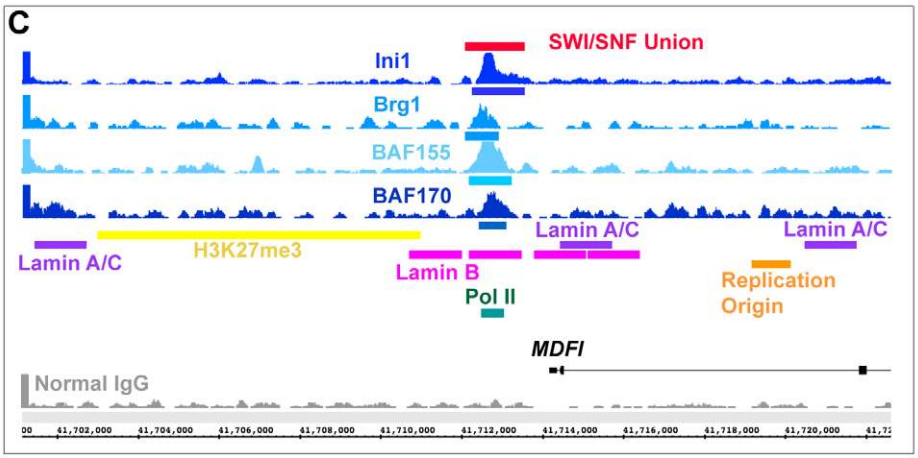
C
SWI/SNF Union
Ini1
Brg1
BAF155
BAF170
Lamin A/C
Lamin A/C
Lamin A/C
H3K27me3
Lamin B
Pol II
Replication Origin
MDFI
Normal IgG

**Figure 1. SWI/SNF regions co-occur with many diverse genomic elements.** The ChIP-Seq regions and signal tracks displayed encompass a ~340 kb region on chromosome 6. The coordinates shown are in hg18 and all regions were identified in HeLa cells as detailed in Table S1 and Materials and Methods. Insets A–D are shown both in the context of the 340 kb region and in magnified view. Inset A displays a ~10 kb region at the edge of a H3K27me3 domain. Inset B displays a ~10 kb region around the 5′ end of *FOXP4*. Inset C displays a ~20 kb region around the 5′ end of *MDFI*. Inset D shows an example of where lamin A/C and lamin B can both flank and overlap with each other. Annotations above the coordinate axis are for forward-strand genes, and annotations below are for reverse-strand genes. Signal tracks are scaled consistently based on number of reads. The vertical axis for each signal track is the count of the number of overlapping DNA fragments at each nucleotide position and is scaled from 0 to 40 for each track.
doi:10.1371/journal.pgen.1002008.g001

ery we asked whether the converse would also be true, namely if regions bound by RNA polymerases are enriched for SWI/SNF. Indeed Pol II regions are enriched for SWI/SNF binding regions ($p<1\times10^{-16}$, GSC test). Although Pol II overlaps extensively with SWI/SNF it differs from SWI/SNF in its concordance with CTCF and enhancer regions (Table S5). Pol II regions lacking SWI/SNF show a five-fold decrease in CTCF sites and a two-fold decrease in enhancer regions as compared to those Pol II regions containing SWI/SNF.

We further compared our SWI/SNF regions with binding intervals identified for RNA polymerase III (Pol III), which in addition to transcribing tRNA and other non-protein coding RNAs has an emerging role in the formation of boundary elements [32,33]. Pol III localization data were obtained from published ChIP-Seq studies using HeLa cells ([34,35]; Tables S1 and S6) and constitute 478 known and novel Pol III-associated regions. Pol II is often associated with Pol III (Table4; reviewed in [32]. Therefore we examined whether SWI/SNF was associated with Pol III binding regions independently of Pol II. Of the 478 Pol III regions, 253 Pol III intervals lack Pol II and among these 39% (98/253) contain one or more SWI/SNF components. These results suggest that SWI/SNF association with Pol III can occur independently of Pol II.

Overall 65% (309/478) of Pol III regions and 84% (19,541/23,320) of Pol II regions have at least one SWI/SNF factor associated with them. The Ini1-BAF155-BAF170 core is found at 41% (195/478) of Pol III regions and 52% (12,079/23,320) of Pol II regions. From the colocalizations of SWI/SNF, Pol II and Pol III we see that there is substantial overlap among these factors yet each of these factors also has distinct characteristics.

## SWI/SNF components bind near many expressed regions

SWI/SNF is known to act as both an activator and repressor of transcription [36]. We examined the locations of four SWI/SNF

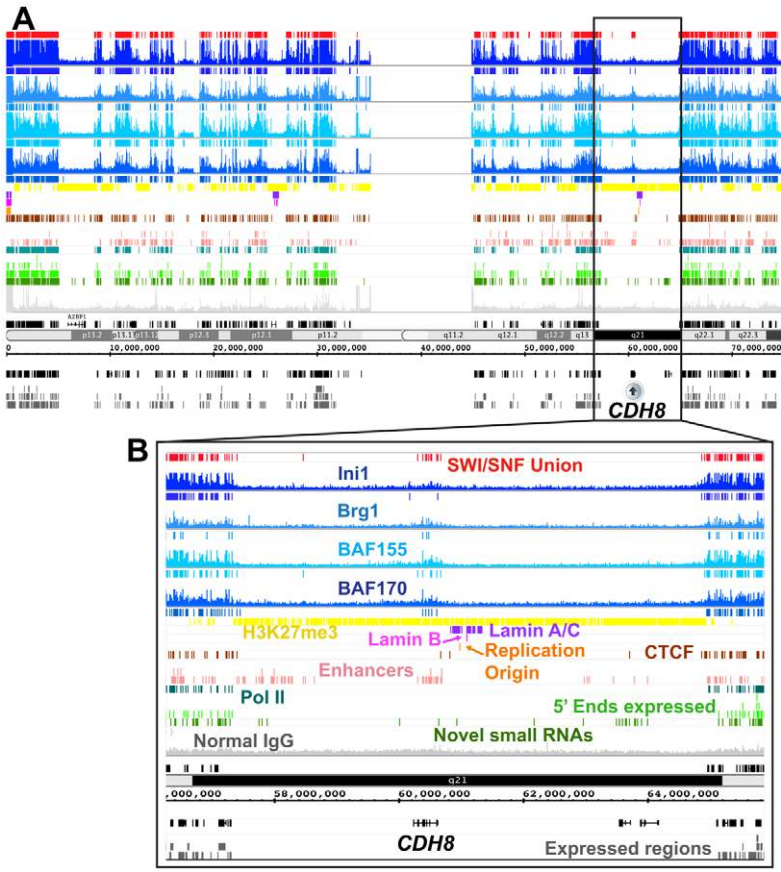


**Figure 2. SWI/SNF signals and target regions in the context of H3K27me3 domains.** As shown in panel A SWI/SNF signals (blue) are sparse in H3K27me3 regions (yellow) along the entire length of chromosome 16. An exception is shown in Panel B where SWI/SNF occurs around the *CDH8* gene that is embedded in a H3K27me3 domain. CDH8 encodes a brain-expressed cadherin that is not expressed in HeLa cells using the data of Morin et al.
doi:10.1371/journal.pgen.1002008.g002

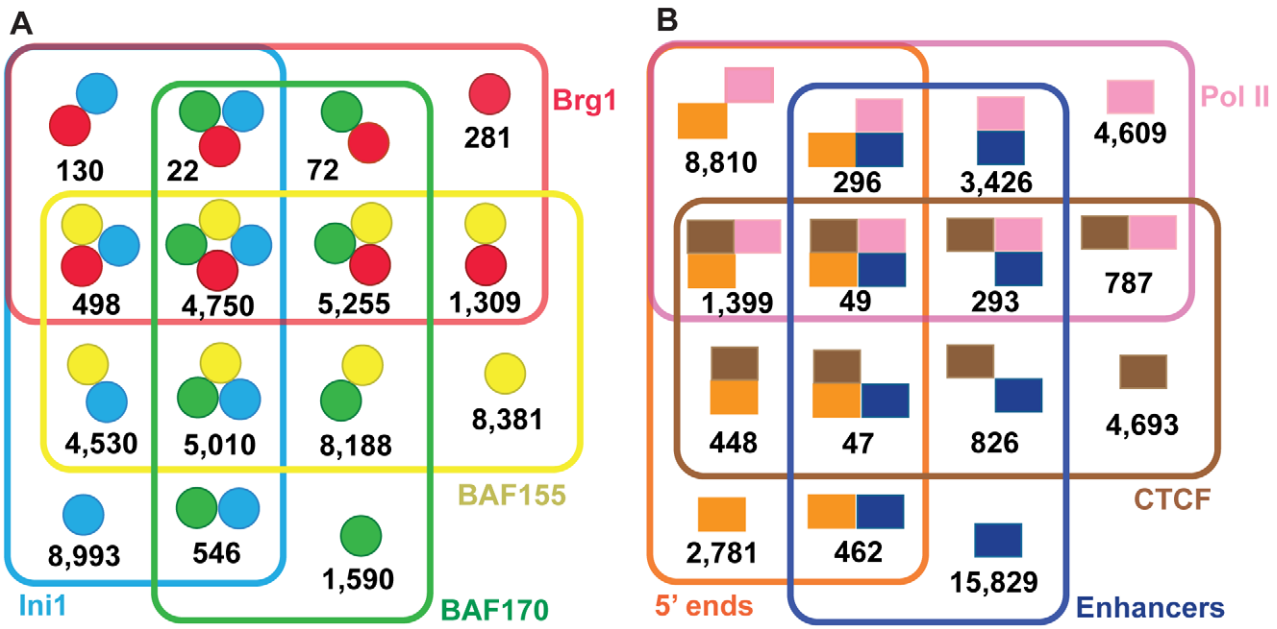


**Figure 3. Venn diagrams showing overlaps for the SWI/SNF union target regions.** Panel A displays the various combinations of all Ini1, BAF155, BAF170 and Brg1 targets in the 49,555 high-confidence union regions (see also Table2). Panel B displays the various combinations of Pol II regions, 5′ ends of Ensembl protein-coding genes, CTCF sites and putative enhancers occurring in the 49,555 SWI/SNF high-confidence union target regions. Of the 49,555 high-confidence union regions, 4,800 (10%) do not contain any of these elements and are defined as "unclassified" (Table3).
doi:10.1371/journal.pgen.1002008.g003

components relative to transcribed regions in HeLa S3 cells using the RNA-Seq data of Morin et al. [37], Ini1, Brg1, BAF155 and/or BAF170 are present at or near the 5′ ends (±2.5 kb) of 71 to 92% of active protein-coding genes. As noted above, SWI/SNF occupancy in promoters is similar to that of Pol II and each of the factors is individually enriched in promoter regions ($p<1\times10^{-16}$, GSC test). Although the majority of Ini1, Brg1, BAF155 and BAF170 target genes are expressed, an appreciable fraction of gene targets have little or no detectable mRNA in HeLa cells. A closer examination of the union regions where a SWI/SNF component is located in the promoter of an inactive gene reveals that 58% (2,063/3,565) of these promoters are co-associated with Pol II suggesting transcriptional stalling (reviewed in [38,39].

Considering that SWI/SNF components bind near many expressed regions and that SWI/SNF factors occur in a multitude of configurations (Figure3 and Table S3), we examined transcript expression levels for all possible combinations of Ini1, Brg1, BAF155 and BAF170 occurrences. Using the RNA-Seq data of Morin et al. [37], we examined transcript expression levels corresponding to each of these configurations (Figure5). We see that the highest levels of transcription are associated with the following four configurations: 1) the complete core of Ini1, BAF155 and BAF170; 2) the complete core plus Brg1; 3) Ini1 and BAF155 only and 4) Brg1, BAF155 and BAF170. Although BAF155 is the subunit that is common to all of the configurations associated with the highest levels of transcription, it does not appear to be the sole driver of transcriptional activity. Compared against each other, all three components of the core complex taken individually have nearly indistinguishable profiles. Despite the involvement of Brg1 in two of the four configurations with the highest expression levels, most other configurations involving Brg1 are restricted to profiles associated with the lowest expression levels. One inference from these data is that certain combinations of SWI/SNF subunits are likely synergistic in promoting transcription whereas other combinations may be inhibitory or unstable.

**Table 2.** Combinations of SWI/SNF factors found in the high-confidence union regions.

| SWI/SNF Union Set | 49,555 |
|---|---|
| Two or more subunits | 30,310 |
| Three or more subunits | 15,535 |
| Core Set: Ini1, BAF155 and BAF170 (may include Brg1) | 9,760 |
| Ini1, BAF155, BAF170 and Brg1 | 4,750 |

doi:10.1371/journal.pgen.1002008.t002

We also examined SWI/SNF occurrences relative to 48,403 non-canonical small RNAs from HeLa cells (≤156 bp; Table S1) where most (83%; $p<1\times10^{-16}$, GSC test) of these small RNAs are near protein-coding genes [40]. Approximately one third (30%) of this entire small RNA set is within 1 kb of a target from our high-confidence union list of 49,555 SWI/SNF regions. The incidence of small RNA-SWI/SNF co-associated regions was nearly equivalent in protein-coding genes and intergenic regions. From this we surmise that SWI/SNF may contribute to gene regulation of a variety of transcripts, many of which are newly annotated and of unknown function.

## SWI/SNF targets genes involved in nuclear function and cancer pathways

Prior research has shown that a variety of signaling cascades are linked to SWI/SNF [25]. To gain further insights into potential actions of SWI/SNF components we examined the underlying Gene Ontology (GO) and Kyoto Encyclopedia of Genes and Genomes (KEGG) designations of their gene targets to determine significantly overrepresented annotations and pathways (Table5 and Table S8). SWI/SNF gene targets were associated with

**Table 3.** Genomic elements found in SWI/SNF target regions.

| Genomic Elements | SWI/SNF union set (49,555 regions total)[1] | SWI/SNF core set (9,760 regions total)[2] |
|---|---|---|
| CTCF, Pol II, Enhancers, 5′ ends (any combination) | 44,755 (90%) | 8,968 (92%) |
| Unclassified | 4,800 (10%) | 792 (8%) |
| RNA Pol II sites | 19,669 (40%) | 6,562 (67%) |
| Putative Enhancers | 21,228 (43%) | 3,431 (35%) |
| CTCF sites | 8,542 (17%) | 1,692 (17%) |
| 5′ ends (within 2.5 kb) of Ensembl protein-coding genes | 14,291 (29%) | 4,089 (42%) |

1 This high-confidence union list is the same described in Table1. For further details see Materials and Methods.
2 The core set is defined as those regions having a co-occurrence of Ini1, BAF155 and BAF170.
doi:10.1371/journal.pgen.1002008.t003

'Pathways in cancer' and several specific cancers types, e.g. chronic myeloid leukemia and pancreatic cancer. A number of signaling pathways and cellular processes that are "hallmarks of cancer" [41] were also overrepresented among the gene targets of Ini1, Brg1, BAF155 and BAF170. These include the Wnt, ErbB, p53, MAPK, and insulin signaling pathways, and processes endemic to oncogenesis and cancer progression such as DNA repair, the cell cycle and apoptosis. From these analyses we surmise the recruitment of SWI/SNF components is likely to influence the molecular basis of cancer through several potential mechanisms.

The SWI/SNF-enriched pathways are highly interconnected. Using the 49,555 SWI/SNF targets we identified a total of 24 KEGG signaling or biochemical pathways (Figure6, yellow nodes). Interestingly, these pathways partition into three groups (Figure6A–6C). Two of the groups (Figure6A and 6B) comprise sets of pathways exhibiting at most one degree of separation, e.g. 'inositol phosphate metabolism' and 'amino sugar and nucleotide sugar metabolism'. The third group (Figure6C) consists of three pathways that are unrelated to any other pathways in the KEGG database. As displayed in Figure S2 directly related pathways such as 'p53 signaling' and the 'cell cycle' have shared components and many of the genes encoding these components are occupied by SWI/SNF factors. Thus, our results demonstrate that SWI/SNF is involved in many closely related signaling pathways and cellular processes and may help serve to coordinate expression of genes involved in these processes.

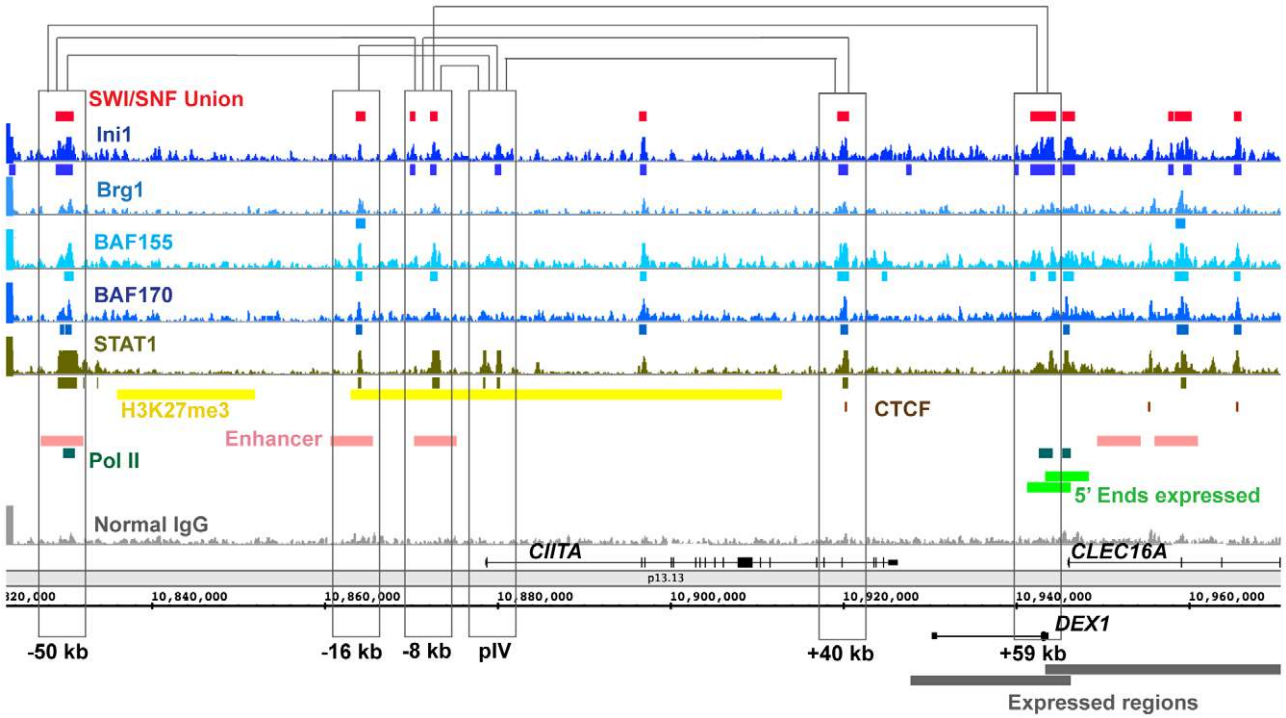


**Figure 4. SWI/SNF signals relative to 3C (Chromosome Conformation Capture) sites in the *CIITA* locus.** A ~150 kb region surrounding the *CIITA* locus is shown with SWI/SNF signals. Chromosomal loops detected in Ni et al. [30] are displayed as brackets connecting regions that were shown to contact each other using 3C. In the absence of γ-interferon eight constitutive contacts have been observed by 3C in HeLa cells between the sites at: (−50:−8), (−50:+59), (−8:+59), (pIV:+40), (−50:pIV), (−16:pIV), (−8:+40) and (−8:pIV). *CIITA* contains STAT1 binding regions; for comparison, STAT1 data are also shown from ChIP-Seq signals and target regions obtained from γ-interferon-stimulated HeLa cells as we previously reported [26]. The Ini1 site at pIV, when joined with BAF155 and BAF170 regions at the −16 kb element, forms complete a SWI/SNF core. The vertical axis for each signal track is the count of the number of overlapping DNA fragments at each nucleotide position and is scaled from 0 to 40 for each track.
doi:10.1371/journal.pgen.1002008.g004

**Table 4.** Co-occurrence of RNA Pol II and Pol III with SWI/SNF high-confidence union regions.

| | All RNA Pol III[1] | All RNA Pol II[2] | SWI/SNF, Pol II and Pol III[3] | SWI/SNF and Pol III present; Pol II absent[4] | Pol III present and SWI/SNF absent[5] | Pol II present and SWI/SNF absent[6] |
|---|---|---|---|---|---|---|
| RNA Pol III | 478 | 182 (0.8%) | 211 | 98 | 169 | 6 (~0.1%) |
| RNA Pol II | 225 (47%) | 23,320 | 211 | 0 | 14 (8%) | 3,779 |
| Ini1 | 274 (57%) | 18,674 (80%) | 201 (95%) | 73 (74%) | 0 | 0 |
| BAF155 | 235 (49%) | 16,175 (69%) | 176 (83%) | 59 (60%) | 0 | 0 |
| BAF170 | 248 (52%) | 12,790 (55%) | 179 (85%) | 69 (70%) | 0 | 0 |
| Brg1 | 75 (16%) | 7,303 (31%) | 68 (32%) | 7 (7%) | 0 | 0 |
| Core | 195 (41%) | 12,079 (52%) | 160 (76%) | 35 (36%) | 0 | 0 |
| CTCF | 49 (10%) | 2,448 (10%) | 14 (7%) | 25 (26%) | 10 (6%) | 68 (<2%) |
| Enhancer | 22 (5%) | 4,527 (19%) | 4 (2%) | 14 (14%) | 4 (2%) | 377 (10%) |
| Protein-coding[7] | 198 (41%) | 18,305 (78%) | 111 (53%) | 34 (35%) | 53 (31%) | 3,052 (81%) |

1 There are a total of 478 Pol III regions genome-wide.
2 There are a total of 23,320 Pol II regions genome-wide.
3 SWI/SNF, Pol II and Pol III co-occur in 211 regions. Percentages shown are relative to these 211 regions.
4 Pol III co-occurs with 98 SWI/SNF regions in the absence of Pol II.
5 Of the total 478 Pol III regions 169 lack SWI/SNF.
6 Of the total 23,320 Pol II regions 3,779 lack SWI/SNF.
7 Regions within 2.5 kb of an Ensembl protein-coding gene.
doi:10.1371/journal.pgen.1002008.t004

## SWI/SNF components associate with proteins involved in multiple aspects of gene regulation and are nodes in a highly integrated network

The genomic binding data demonstrates that SWI/SNF localization is coupled with a broad range of functional elements, suggesting that SWI/SNF may also be found with a broad range of associated proteins. To further examine the scope of SWI/SNF's roles in the nucleus we analyzed proteins associated with SWI/SNF subunits using co-immunoprecipitation followed by mass spectrometry. The SWI/SNF components Ini1, BAF155,

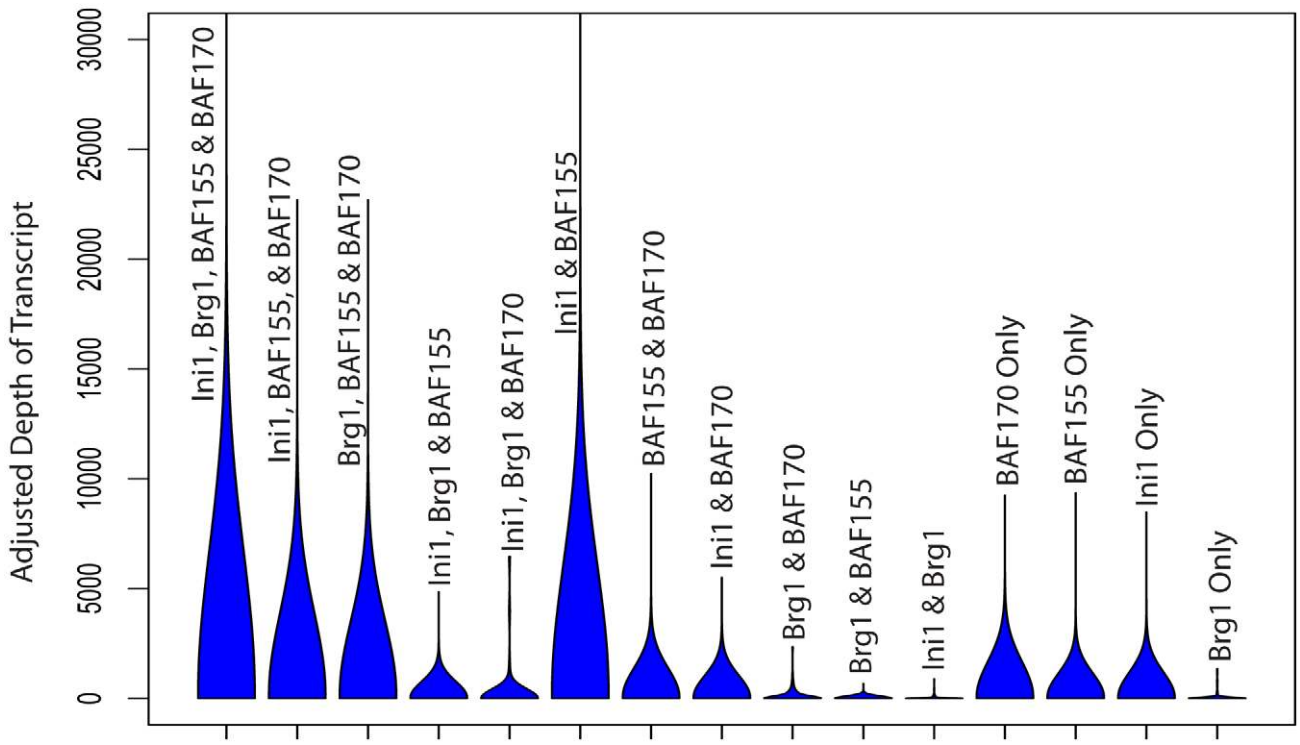


**Figure 5. Violin plots of expression values across all possible SWI/SNF subunit occurrences.** Violin plots display the probability density function plotted against the adjusted depth (i.e. expression) values from Morin et al [37]. Transcript counts for each category are given in Table S7. We find that some combinations of subunits are associated with transcripts with higher expression levels while other combinations are associated with transcripts with lower expression levels.
doi:10.1371/journal.pgen.1002008.g005

**Table 5.** Significant pathways and biological processes associated with SWI/SNF union ChIP-Seq regions.

| Overrepresented categories for the SWI/SNF union regions[1] | Benjamini-corrected p-values |
|---|---|
| KEGG hsa05200:Pathways in cancer | $4.7\times10^{-8}$ |
| KEGG hsa05212:Pancreatic cancer | $4.9\times10^{-3}$ |
| KEGG hsa05222:Small cell lung cancer | $1.7\times10^{-3}$ |
| KEGG hsa05211:Renal cell carcinoma | $2.5\times10^{-3}$ |
| KEGG hsa05220:Chronic myeloid leukemia | $3.4\times10^{-4}$ |
| KEGG hsa05215:Prostate cancer | $8.9\times10^{-3}$ |
| KEGG hsa05210:Colorectal cancer | $1.7\times10^{-3}$ |
| KEGG hsa05016:Huntington's disease | $2.1\times10^{-4}$ |
| KEGG hsa05010:Alzheimer's disease | $1.4\times10^{-3}$ |
| KEGG hsa04010:MAPK signaling pathway | $1.3\times10^{-5}$ |
| KEGG hsa04012:ErbB signaling pathway | $2.6\times10^{-3}$ |
| KEGG hsa04115:p53 signaling pathway | $3.4\times10^{-4}$ |
| KEGG hsa04310:Wnt signaling pathway | $7.8\times10^{-3}$ |
| KEGG hsa04910:Insulin signaling pathway | $8.9\times10^{-3}$ |
| KEGG hsa04070:Phosphatidylinositol signaling system | $7.9\times10^{-3}$ |
| KEGG hsa04120:Ubiquitin mediated proteolysis | $8.4\times10^{-7}$ |
| KEGG hsa03040:Spliceosome | $8.6\times10^{-10}$ |
| GO:0051056 regulation of small GTPase mediated signal transduction | $1.8\times10^{-3}$ |
| GO:0007049 cell cycle | $3.4\times10^{-34}$ |
| GO:0006260 DNA replication | $4.5\times10^{-10}$ |
| GO:0051301 cell division | $4.1\times10^{-18}$ |
| GO:0006281 DNA repair | $5.6\times10^{-20}$ |
| GO:0006915 apoptosis | $8.8\times10^{-9}$ |
| GO:0051276 chromosome organization | $1.5\times10^{-11}$ |
| GO:0016568 chromatin modification | $2.1\times10^{-17}$ |
| GO:0006357 regulation of transcription from RNA polymerase II promoter | $6.1\times10^{-7}$ |
| GO:0034470 ncRNA processing | $2.4\times10^{-15}$ |
| GO:0001701 in utero embryonic development | $1.5\times10^{-5}$ |

1 Overrepresented terms were determined using DAVID tools for Ensembl genes corresponding to the 49,555 SWI/SNF union regions for Benjamini corrected p-values<0.01. A complete list is available in Table S7.
doi:10.1371/journal.pgen.1002008.t005

BAF170, Brg1, Brm and ARID1A were immunoprecipitated from HeLa S3 nuclei, the resulting proteins were gel-separated and peptides were generated for analysis by mass spectrometry (See Materials and Methods; Table S9). In addition to the factor-specific antibodies, parallel immunoprecipitations were performed using non-specific IgG antibodies. Proteins identified in these "control IgG" immunoprecipitations were excluded as potential SWI/SNF co-purifying factors.

We identified a total of 101 proteins that were specifically associated with at least one of the SWI/SNF components assayed (Figure7, turquoise edges; Table S10). Of the non-SWI/SNF subunits detected, 5 of these interactions were found previously in HeLa cells (e.g. estrogen receptor alpha [42], and 96 were new to this study. Interestingly one of the novel interactions we observed in HeLa cells, BAF155 with NUF2, has been previously observed in yeast between the yeast homolog of BAF155 (SWI3) and NUF2 [15]. Using the 101 nodes that we identified as proteins co-purifying with SWI/SNF in our undirected approach we ascertained overrepresented GO categories (Table6). Several of these designations such as 'cell cycle' and 'chromosome organization' coincide with the categories obtained from GO and pathway analyses of SWI/SNF ChIP-Seq targets, suggesting the possibility of highly-interactive network structures.

Many of the proteins that were novel to this study reinforce and expand upon other published reports of SWI/SNF characterizations. For example SWI/SNF components have been localized by immunofluorescence to mitotic kinetochores and spindle poles [43], and Brg1-deficient mice show dissolution of pericentromeric heterochromatin domains [44]. From our immunoprecipitations BAF155 and BAF170 were associated with a number of kinetochore and centrosomal proteins (e.g. BUB1B, CENPE and NUF2, Figure8, green circles). The role of SWI/SNF in the maintenance of kinetochore and spindle function is unknown. We detected a variety of transcription factor activators and repressors (e.g. NFκB1, NFκB2, RelA, PML and NFX1) as well as DNA repair (ERCC5 and RAD50) and cell cycle (e.g. CCNB3 and CDCA2) proteins (Figure S3). Some of the SWI/SNF interacting proteins themselves interact with one another. For example we detected several different proteins integral to estrogen and insulin signaling (Figure7; Table S10). We also identified proteins associated with only one SWI/SNF factor; these may either be interactions with a specific SWI/SNF component or an inability to detect the protein in the immunoprecipitations.

We developed an expanded network of SWI/SNF associations by including proteins that were found by others to co-purify with SWI/SNF subunits (Figure7, black edges). Only those factors that showed a one-degree separation with a SWI/SNF component in HeLa cells are displayed and all interactions are annotated in Table S10. SWI/SNF interacting proteins are associated with numerous UniProt keywords (Figure8; [45]). Overall these results suggest a role for SWI/SNF components in a wide array of nuclear processes and diseases. Some of these processes may take place in nuclear substructures. Higher order chromatin structure is facilitated by the nuclear lamina and tethering of genes to the nuclear periphery is one epigenetic mechanism of gene regulation [46,47]. Intriguingly we and others have detected SWI/SNF components with various nuclear envelope-associated proteins (Figure7 and Table S10) including lamin A, EMD (emerin) and BAF/BANF1 (Barrier to Autointegration Factor, which although similar in name is not a SWI/SNF subunit). Two of the nuclear membrane proteins, SYNE1 and C14orf49, that we isolated in association with BAF155 are part of LINC complexes that link the nucleoskeleton and cytoskeleton [48,49].

## A fraction of SWI/SNF regions are associated with the nuclear lamina

Numerous studies point to a high degree of functional organization in cell nuclei [46]. Emerging nuclear organization models would benefit greatly from a catalogue of processes and chromatin characteristics mapped to particular genomic elements. For example, the nuclear lamins are thought to influence chromatin organization, DNA replication and transcription [47,50]. Our immunoprecipitation results demonstrating that SWI/SNF components are associated with lamin A/C (Figure7 and Table S10) along with immunoprecipitation, immunolocalization and cell fractionation experiments from others demonstrating an association between SWI/SNF and nuclear lamina (e.g. emerin Figure7; [51]) prompted us to investigate whether SWI/SNF and the lamins can be located to the same genomic sequences.

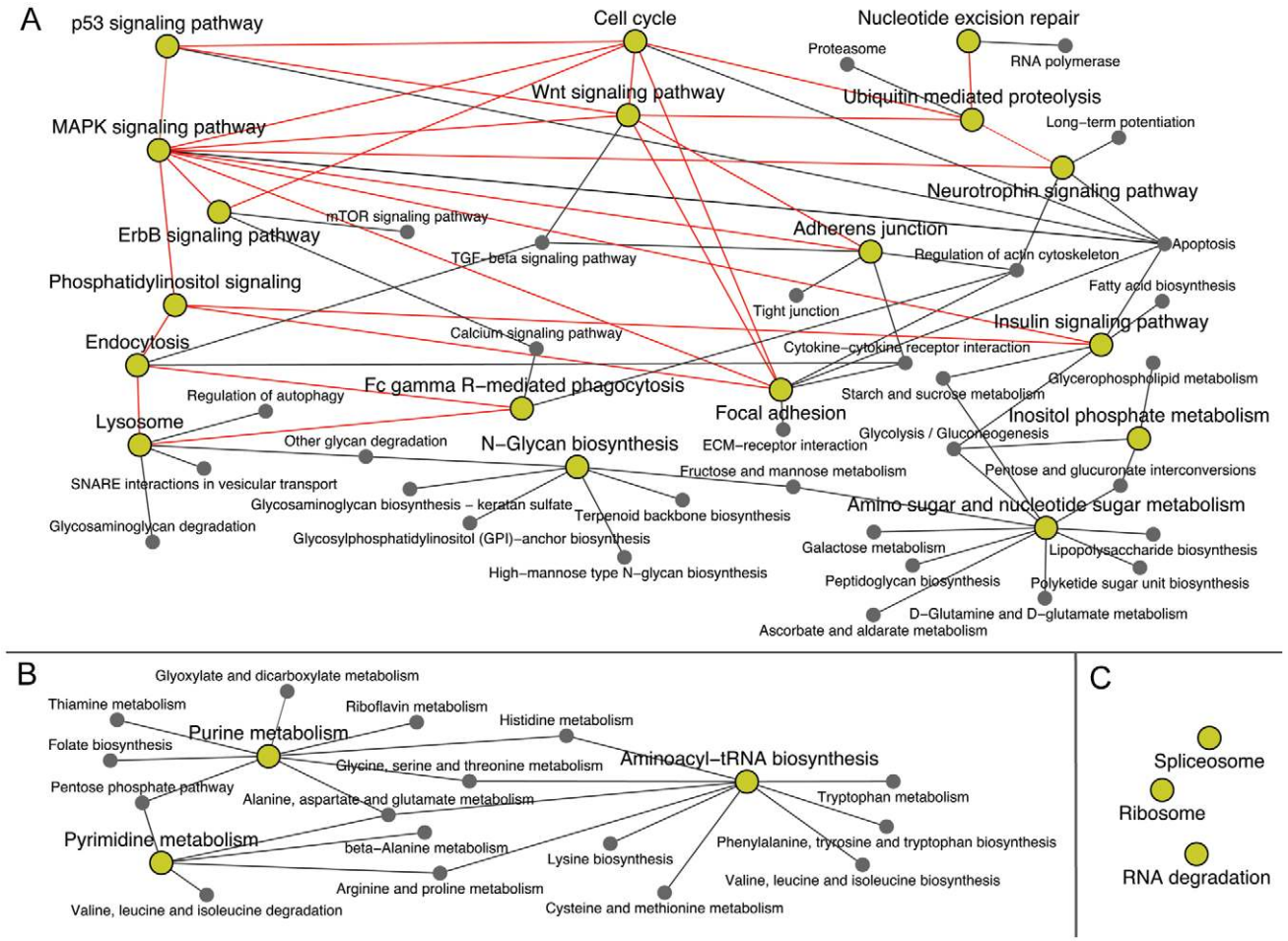


**Figure 6. Network of overrepresented and other related KEGG pathways identified using SWI/SNF ChIP-Seq union regions.** The KEGG pathways identified as overrepresented using the 49,555 SWI/SNF ChIP-Seq union regions are shown as yellow nodes and each of their related, KEGG-designated pathways are also displayed. Pathways related to the overrepresented pathways but that are not overrepresented themselves are shown as gray nodes. Red edges connect yellow nodes. Three of the nodes, spliceosome, ribosome and RNA degradation, are distinct and unrelated to other pathways according to the KEGG database. From this analysis three groups of pathways emerged: A) pathways related to signal transduction, glycan and carbohydrate metabolism, cell growth and death and other cellular processes B) nucleotide and amino acid metabolism and C) genetic information processing.
doi:10.1371/journal.pgen.1002008.g006

We isolated lamin A/C and lamin B ChIP DNA from HeLa S3 nuclei and performed ChIP-chip on tiling arrays covering the ENCODE pilot regions (see Materials and Methods and Table S1). Most of the 1,770 lamin A/C regions mapped to H3K27me3 domains (76%; 1,337/1,770) whereas the 1,270 lamin B regions were less commonly associated with H3K27me3 (29%; 372/1,270). Comparing regions where signal was detectable for the SWI/SNF, lamin A/C and lamin B experiments revealed that SWI/SNF has a much higher overlap with lamin B than lamin A/C. We found that 38% (297/784) of SWI/SNF sites are within 100 bp of a lamin B region whereas only 5% (41/784) of SWI/SNF sites are within 100 bp of a lamin A/C region (Table7). For both lamin types the colocalization with SWI/SNF regions is significant relative to random target lists (lamin B, $p<1\times10^{-16}$; lamin A/C, $p<1\times10^{-15}$; GSC tests). SWI/SNF-lamin B intersecting regions contained approximately the same proportion of CTCF sites in the ENCODE regions as did all SWI/SNF sites in the ENCODE regions ($p>0.05$ hypergeometric test; Table7). Enhancers are underrepresented in the SWI/SNF-lamin B regions relative to all SWI/SNF locations in the ENCODE regions ($p<1.9\times10^{-36}$; hypergeometric test). The SWI/SNF-lamin B regions are overrepresented for Pol II ($p<2.9\times10^{-39}$; hypergeometric test) and 5′ ends ($p<7.3\times10^{-37}$; hypergeometric test) relative to all SWI/SNF locations in the ENCODE regions.

In crosslinked chromatin SWI/SNF is detected primarily with lamin B, but as noted from the above mass spectrometry experiments, in solubilized, non-cross-linked cells SWI/SNF is detected with lamin A/C and not lamin B (Figure1 and Figure7). We interpret these results to indicate that SWI/SNF, lamin A/C and lamin B co-associate in different nuclear contexts but are all part of a broader interacting network with specific sub-associations.

## Association of SWI/SNF with DNA replication origins

SWI/SNF and the lamins have each been implicated in DNA replication (see above; [52,53]). One of the proteins we detected as associated with SWI/SNF is the replication protein RepA and another regulator of DNA replication, geminin, has been found to co-purify with SWI/SNF in HeLa cells (Figure7, red circles; [54]). We investigated whether there might be a relationship among SWI/SNF, lamins and DNA replication origins. We obtained a set of 282 DNA replication origins identified in HeLa cells for the

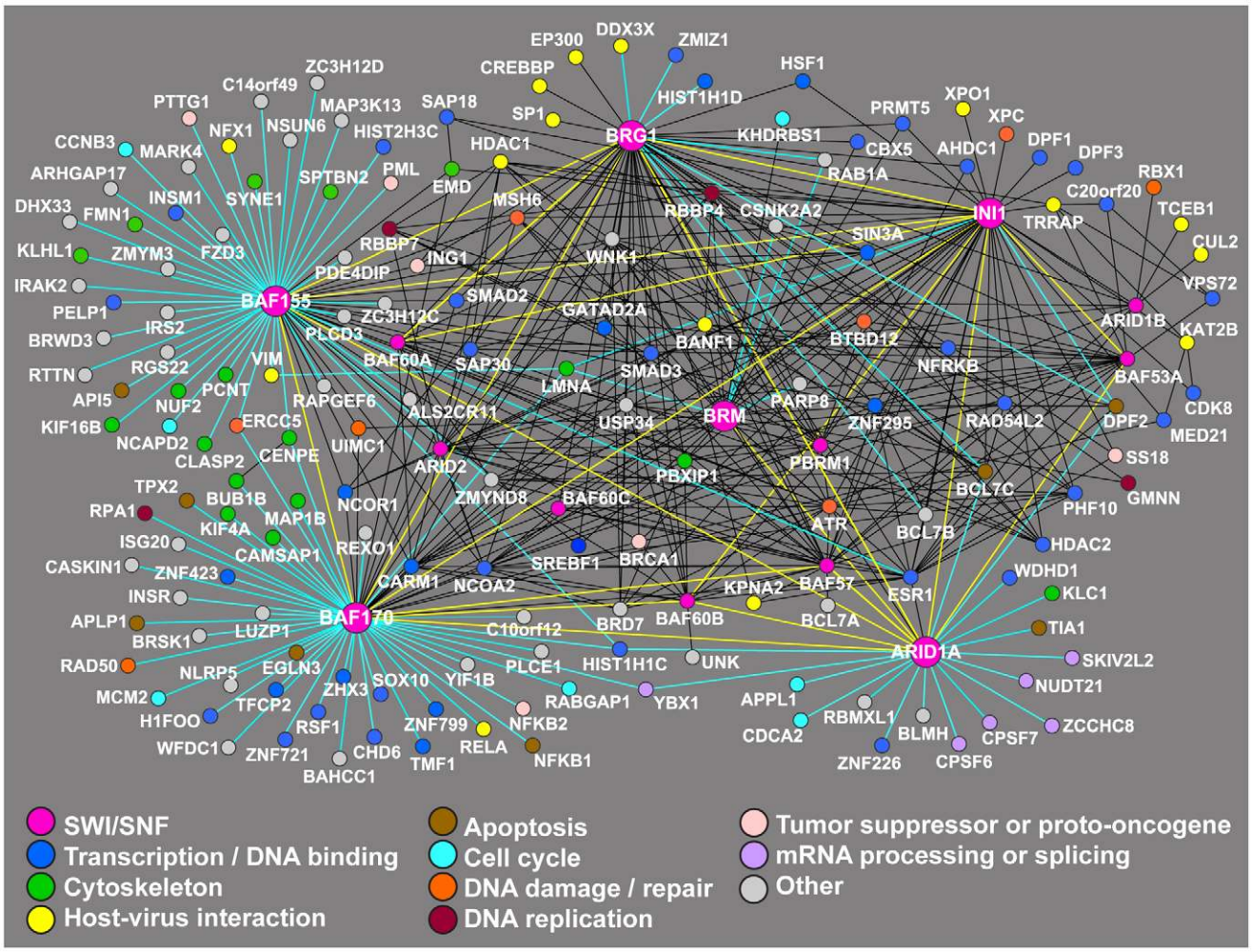


**Figure 7. Network of proteins that have been shown to co-purify with SWI/SNF factors.** 158 proteins have been shown to co-purify with SWI/SNF factors in HeLa cells, either by our IP-mass spectrometry experiments or in other studies. Interactions are annotated in Table S10. As indicated in the figure key, pink circles denote SWI/SNF components; the larger pink circles are SWI/SNF factors used as bait in this study. Blue edges denote interactions detected in this study. Yellow edges indicate interactions between SWI/SNF factors themselves that were detected in this study. Black edges indicate interactions from other published sources. As noted in Table S10, the studies used a variety of biochemical methods and SWI/SNF factors were either bait or prey. Non-SWI/SNF factors are color-coded according to UniProt keywords [45].
doi:10.1371/journal.pgen.1002008.g007

ENCODE regions ([55]; Table S1). Of these 282 replication origins, 90 (32%) occur within 100 bp of a SWI/SNF region ($p<1\times10^{-16}$, GSC test), 86 (31%) occur at the 5′ ends of protein-coding genes and 151 (54%) occur within 100 bp of a lamin B region. In contrast to lamin B, only 17% (48/282) of the replication origins were near a lamin A/C region. These results are consistent with nuclear staining patterns observed in mouse 3T3 cells showing colocalization between lamin B and sites of DNA replication whereas the same colocalization patterns were not observed for replication foci and lamin A [52].

Of the 86 replication origins in promoter regions, 88% (76/86) intersected a lamin B region and most (78% or 67/86) were within a 100 bp of a SWI/SNF region. These data indicate that SWI/SNF components are located near many DNA replication origins, particularly those located in promoter regions. The coincidence of chromatin remodeling factors, promoters, lamins and replication origins at the same subset of genomic regions suggests that these loci may be particularly favorable for the formation of both DNA and RNA polymerase assembly and chromatin tethering. As shown in Figure1 the interplay among these elements as well as with Pol II, CTCF and heterochromatin regions is complex and interwoven, such that each may share many different supporting and counteracting roles.

## Discussion

SWI/SNF performs a crucial function in gene regulation and chromosome organization by directly altering contacts between nucleosomes and DNA. In the work presented here we undertook a two-pronged approach (ChIP-Seq and IP-mass spectrometry) to move towards a more thorough understanding of these functions. Our ChIP-Seq analyses demonstrate that SWI/SNF components overlap extensively with important regions that require tight control of the dynamics of nucleosome occupancy such as promoters, enhancers and CTCF sites. Not only does the SWI/SNF complex change the accessibility of DNA but it also acts in concert with an extensive host of cooperating factors, thereby facilitating combinatorial control among various genomic elements. In addition to our ChIP-Seq results, the diversity and number of proteins that co-purify with SWI/SNF as identified in

**Table 6.** Over-represented annotations from proteins identified as co-purifying with SWI/SNF in this study.

| Overrepresented categories for SWI/SNF co-associated proteins[1] | Benjamini-corrected p-values |
|---|---|
| GO:0007049 cell cycle | $3.8\times10^{-4}$ |
| GO:0000279 M phase | $2.8\times10^{-4}$ |
| GO:0015630 microtubule cytoskeleton | $8.4\times10^{-4}$ |
| GO:0006323 DNA packaging | $7.9\times10^{-3}$ |
| GO:0000793 condensed chromosome | $8.1\times10^{-3}$ |
| GO:0051276 chromosome organization | $9.9\times10^{-3}$ |
| GO:0006333 chromatin assembly or disassembly | $1.0\times10^{-2}$ |
| GO:0005813 centrosome | $1.2\times10^{-2}$ |
| GO:0034728 nucleosome organization | $1.5\times10^{-2}$ |
| GO:0005815 microtubule organizing center | $2.2\times10^{-2}$ |
| GO:0016584 nucleosome positioning | $2.8\times10^{-2}$ |
| GO:0000777 condensed chromosome kinetochore | $2.9\times10^{-2}$ |

Overrepresented terms were determined using DAVID for Ensembl genes corresponding to the 101 proteins we identified as co-associated with a SWI/SNF factor as determined by IP-mass spectrometry. We considered Benjamini-corrected p-values$<$0.05. A complete list is available in Table S8.
doi:10.1371/journal.pgen.1002008.t006

our mass spectrometry experiments further supports SWI/SNF's involvement with a variety of functionally distinct complexes.

RNA polymerases II and III are extensively colocalized with SWI/SNF components. Studies of transcription in HeLa cells have estimated that the number of active RNA II polymerases exceeds the number of transcriptionally active sites by at least one order of magnitude, leading to the proposal of "transcription factories" [1–3]. The number of RNA Pol II transcription factories in HeLa cells has been estimated between 5,000 and 8,000 where each factory can be typified by several looped loci, their resulting transcripts and distal elements such as enhancers. We infer that SWI/SNF regions are prevalent in transcriptional assemblages and their associated regulatory loops, given that $>$90% of our high-confidence union targets are associated with genic or regulatory regions and that 65% of Pol III and 84% of Pol II regions colocalize with at least one SWI/SNF factor (Table4, Tables S5 and S6).

Interestingly we observed that SWI/SNF components often occur independently of each other and in various configurations across the genome, and similarly our mass spectrometry data point to heterogeneity of SWI/SNF complexes. We speculate that several mechanisms may underlie these various configurations and their associated genomic features, including 1) synergism or antagonism of the individual SWI/SNF factors in influencing expression (e.g. Figure5); 2) failure to detect individual subunits due to epitope masking as a consequence of variation with local environments; 3) the capture of incomplete complexes that may in fact be completed upon superposition of genome-wide 3C data once such data become available (e.g. Figure4); 4) the existence of SWI/SNF sub-complexes that deviate from the conventional composition of SWI/SNF assemblies (e.g. [56]) or 5) the capture of intermediates in a multistep assembly or remodeling process. This last view is consistent with a model of stochastic assembly that may occur through intermediate interactions and that has been described for several other large, multifactor complexes such as RNA polymerases and associated transcription factors [57], spliceosomes [58], and DNA repair complexes [59].

As shown in Figure6 SWI/SNF occurs throughout many interconnected pathways. The assembly of functional SWI/SNF complexes at many locations in the genome may require the activation of one or more of these related pathways. Consequently some of the SWI/SNF associated regions we observed may reflect constitutive binding of partially assembled complexes that may be poised to receive additional signal inputs for subsequent regulatory activity. Indeed it has been shown that SWI/SNF components are present at regulatory regions even in the absence of stimulatory conditions or tissue-specific cofactors. For example Brg1 is present constitutively at the interferon-inducible genes *IFITM3* [60] and *CIITA* [30] in unstimulated HeLa cells, which is consistent with our own finding of Brg1 and Ini1 at *IFITM3* and various combinations of BAF155, BAF170, Ini1 and Brg1 at different elements in *CIITA*. In solution SWI/SNF factors are associated constitutively with RelB (HEK293 cells, [61]), RelA, NFkB1 and NFkB2 (HeLa cells, this study), the glucocorticoid receptor (T4D7 cells, [62]) and estrogen receptor alpha (HeLa cells, this study and [42]; SW13 cell extracts, [63]). The prevalence of SWI/SNF and the high degree of connectivity of its overrepresented pathways implies that SWI/SNF may assist in many related processes and may even facilitate crosstalk across many constituents of the transcriptional machinery. Notably SWI/SNF binds in the genes of its own subunits (Table S19) suggesting that SWI/SNF may contribute to auto- and cross-regulation of its subunit levels. Loss-of-function of a particular subunit, as may occur in certain cancers, could initiate oscillations and alter the relative abundance of the levels of the other SWI/SNF subunits through a variety of feedback and feed-forward loops. Aberrant SWI/SNF expression has been proposed to result in new combinatorial assemblies of SWI/SNF, some of which may deleterious [64].

The gene attributes revealed by our ChIP-Seq data substantiate that SWI/SNF is proximal to targets that comprise sets of fundamental biological processes. Many of the functional categories we found to be significantly overrepresented have disease implications, especially as related to cancer (Figure S2). For example failures in DNA repair and unchecked cell cycle activity are common characteristics of pre-cancerous cells, and our SWI/SNF analyses identified the p53 and MAPK signaling pathways, which are well known for maintaining checkpoint functions. Growth dysregulation particularly in the context of hormone signaling is another common cancer phenotype. Extracellular growth signals are transduced from the cell membrane to the nucleus by the ErbB, insulin and phosphtidylinositol signaling pathways, all of which we recovered as overrepresented (Table5). The existence of phosphoinositide signaling in the nucleus and the ability of Brg1 to act as an effector for phosphatidylinositol 4,5-bisphosphate ($PIP_2$) raises the prospect of several levels of control of this signaling pathway with respect to SWI/SNF [65], a hypothesis that can be examined in future studies.

Several of the overrepresented pathways we identified through our ChIP-Seq analyses share proteins detected in SWI/SNF co-purification experiments, thereby providing a resource to explore potential, highly-interactive network structures. For example we found that genes with products critical for 'nucleotide excision repair' were enriched using our SWI/SNF union list (Figure6). Within this pathway the excision repair protein ERCC5 co-purified with both BAF155 and BAF170 in our IP (immunoprecipitation)-mass spectrometry experiments. The excision repair protein, XPC, associates with SWI/SNF in response to UV irradiation in HeLa cells, and BRCA1 and ATR also cooperate with SWI/SNF in DNA repair (Figure7; Table S10; [66]). Thus we speculate SWI/SNF may participate in DNA repair through both transcriptional regulation as well as recruitment to regions undergoing repair.

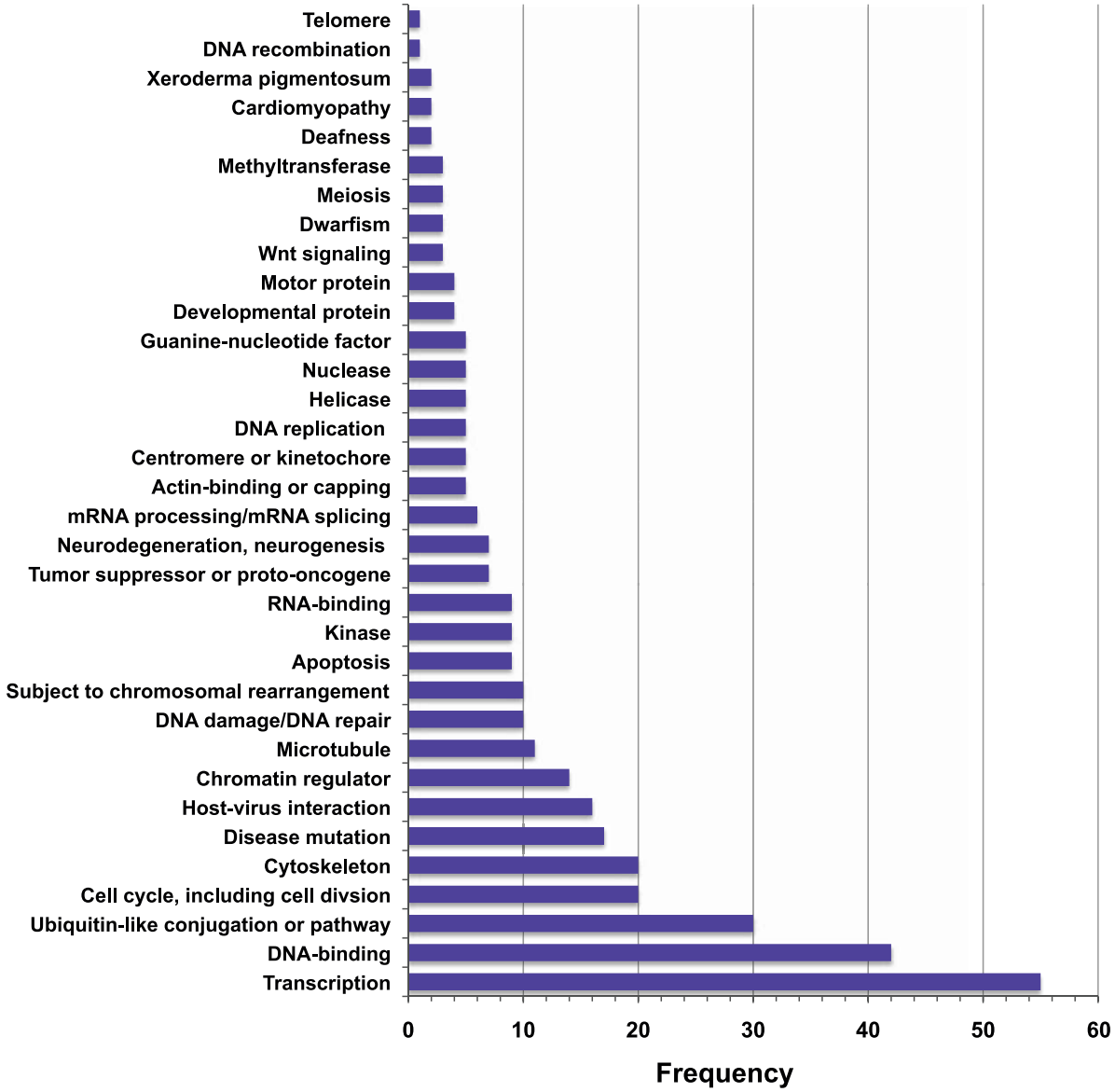


**Figure 8. Histogram showing the frequencies of UniProt keywords for proteins that co-purify with SWI/SNF factors.** Keywords shown were retrieved from the UniProt database [45] for proteins that co-purify with a SWI/SNF factor, as annotated in Table S10.
doi:10.1371/journal.pgen.1002008.g008

Our study uses two strategies to attempt to comprehensively collect a SWI/SNF interaction network. We limited our network to a single model system, HeLa cells, because many attributes of SWI/SNF have been documented in these cells and it has been noted that SWI/SNF associations vary by cell type [67]. We extensively collated SWI/SNF protein interactions described in the literature. This undertaking was necessary because many of the proteins described in the literature as co-associated with SWI/SNF factors are not represented in interaction databases such as BioGRID, Molecular Interactions Database (MINT), IntAct, Human Protein Reference Database (HPRD), Nuclear Protein Database (NPD) and Interologous Interaction Database (I2D). Therefore we attempted to comprehensively collect such information to overcome these limitations. In total 158 SWI/SNF interacting proteins have been described in HeLa cells (Figure8 and Table S10), which is similar to the number of SWI/SNF interacting proteins that have been described in other cell types [67]. Published molecular associations that were not discerned here might be due to interactions that are: 1) transient or of low affinity, 2) dependent on a specific set of biochemical conditions or 3) undetectable due to masking by the presence of more abundant protein(s) of similar size. In working with protein interaction data, similar degrees of overlap have been noted when comparisons are made across data sets [68,69] and even in a well-studied model such as yeast, mass spectrometry analyses have found a plasticity of complexes and many previously undetected interactions [70–72]. From the ChIP-Seq and ChIP-chip results we expected that CTCF and lamin B may be among the proteins that co-associate with SWI/SNF, however neither of these factors was recovered in any of the non-directed experiments (Table S10), including a CTCF immunoprecipitation-mass spectrometry experiment performed in HeLa cells. In addition to the above considerations one possibility is that CTCF or lamin B may associate more strongly with one of the SWI/SNF factors not studied, e.g. BAF53A or one of the BAF60 subunits.

**Table 7.** Co-occurrence of SWI/SNF factors and lamins in the ENCODE regions.

| | Lamin A/C[1] | Lamin B[2] | SWI/SNF[3] |
|---|---|---|---|
| Ini1 | 22 (54%) | 186 (63%) | 598 (76%) |
| Brg1 | 6 (15%) | 75 (25%) | 204 (26%) |
| BAF155 | 31 (76%) | 216 (73%) | 588 (75%) |
| BAF170 | 23 (56%) | 155 (52%) | 394 (50%) |
| CTCF | 7 (17%) | 60 (20%) | 146 (19%) |
| Enhancers | 8 (20%) | 32 (11%) | 289 (37%) |
| RNA Pol II | 23 (56%) | 214 (72%) | 335 (43%) |
| 5′ Ends | 15 (37%) | 186 (63%) | 274 (35%) |
| 5′ Ends, expressed | 12 (29%) | 128 (43%) | 93 (12%) |
| 5′ Ends, not expressed | 4 (10%) | 66 (22%) | 191 (24%) |

1 A total of 41 SWI/SNF regions intersect a lamin A/C region.
2 A total of 297 SWI/SNF regions intersect a lamin B region.
3 There are 784 SWI/SNF high-confidence union regions that were used for comparison with lamin ChIP-chip array data.
doi:10.1371/journal.pgen.1002008.t007

SWI/SNF is most often described in a chromatin remodeling context however data derived from a variety of sources suggests that SWI/SNF has other facets. It is possible that not all of SWI/SNF's functions involve DNA localization and therefore other types of global experiments, such as the IP-mass spectrometry, are valuable as first steps towards recognizing previously unknown roles. Unlike cytoplasmic compartments, nuclear compartments are not separated by a physical barrier but rather are functional assemblies that are typically organized around sets of molecules engaged in common functions. Data from both ChIP-Seq and IP-mass spectrometry illuminate the sectors in which SWI/SNF operates and the integration of these two methods is better than each alone for furnishing a broad comprehension of SWI/SNF action. For example ChIP-Seq enables the global identification of SWI/SNF chromosomal elements except for those regions with highly repetitive sequence such as human centromeres (Figure2A). In this respect IP-mass spectrometry is complementary to ChIP-Seq because it strongly suggests that SWI/SNF occurs at kinetochores as evidenced by its co-purification with CENPE, NUF2, BUB1B and CLASP2 (Figure7 and Figure9). In addition to kinetochore proteins the SWI/SNF co-purification experiments also uncovered proteins from other substructures including centrosomes, microtubules, the nuclear periphery and PML nuclear bodies, the latter of which is characterized by cryptic foci of PML (promyelocytic leukemia protein) and has been implicated in a variety of diseases [73]. The ChIP-Seq and IP-mass spectrometry data are synergistic as well. Notably both methods found an overrepresentation of regions or proteins enriched for 'cell cycle' and 'chromosome organization'. One possible inference from these studies is that SWI/SNF is well positioned to integrate signals across multiple signaling pathways both by its presence in a variety of cellular structures and its role in gene regulation through chromatin remodeling.

A fraction of SWI/SNF complexes co-associate with elements of the nuclear periphery where they are well situated to contribute to the nuclear organization and position-dependent gene expression (Figure7; [74]). We found that in crosslinked cells SWI/SNF localizes more widely with lamin B than lamin A whereas in non-crosslinked cells SWI/SNF co-purifies with lamin A. As mentioned above lamin B may have escaped detection in SWI/SNF protein interaction studies. A related possibility is that SWI/SNF may exist in different nuclear pools that have varying solubilities and associations, such that recovery of particular SWI/SNF complexes depends upon the proteins with which SWI/SNF is associated. For example lamins A and B are known to have different nucleoplasmic mobilities and localization patterns [50,52]. Immunolocalization experiments in HeLa nuclei have revealed that the A/C- and B-type lamins form distinct meshworks with occasional points of intersection [50], which is consistent with the interspersed patterns of lamin A/C and B that we detected (Figure1). Hence it is reasonable to expect that SWI/SNF associated with lamin A would behave differently than when associated with lamin B. We surmise that in a chromatin context the dominant association of SWI/SNF with the nuclear lamins occurs in regions where lamin B is present. The purification of SWI/SNF with lamin A may indicate other biological roles, such as cell cycle progression or nuclear assembly [75,76].

Gaining a more detailed understanding of SWI/SNF's activities in or near various heterochromatin environments will be central to comprehending nuclear events over the cell cycle as well as during development. Among the numerous molecular and epigenetic factors that have been found to affect heterochromatin formation or maintenance, the heterochromatin protein 1 alpha (HP1α, also known as CBX5; Figure7) and Polycomb complexes (PcG) are of particular relevance to SWI/SNF [77–79]. Polycomb complexes promote gene silencing by catalyzing the trimethylation of H3K27 in its target regions, and SWI/SNF antagonizes this epigenetic silencing [80]. It is tempting to speculate that SWI/SNF found near the edges of H3K27me3 domains (Figure1A and 1C) may be contributing to the establishment or maintenance of boundary elements. SWI/SNF may also engage in heterochromatin dynamics through its interaction with HP1α, which is often located in the centromeric regions (reviewed in [81]). Curiously HP1α interacts with the lamin B receptor [82] thus providing a potential bridge between heterochromatin and the inner nuclear membrane. Both H3K27me3 and lamin B are associated with spatially regulated genes whose conversion between active and inactive states depends on access to their regulatory regions, as may be conferred by SWI/SNF.

The work presented here provides new insights into the scope of SWI/SNF's influence in gene regulation and nuclear organization. The integration of numerous studies is beginning to reveal the complexities contributing to the regulation of any given locus. Contemporary models of transcriptional control propose that a series of factors transiently associate with a regulatory region before a decisive event tilts these intermediate reactions towards a productive outcome [57,83]. SWI/SNF may contribute to such intermediate reactions or trigger switches between inactive and active states. The capacity for SWI/SNF to preserve many aspects of homeostasis also makes it vulnerable to being ensnared for aggressive cell proliferation. Our work demonstrates that SWI/SNF in particular and perhaps chromatin remodeling proteins in general will contribute unique insights to our understanding of gene regulation and disease mechanisms through the integration of target regions, spatial positioning and functional annotations. For example the co-occurrence of SWI/SNF with centrosomes, microtubules, kinetochores and the nuclear periphery may suggest that a pool of SWI/SNF is sequestered by these structures during mitosis to assist in the post-mitotic reformation of chromosomal territories. Our collective findings help inform a comprehensive view of SWI/SNF function as well as form a valuable compendium for future studies of nuclear functions as related to chromatin remodeling.

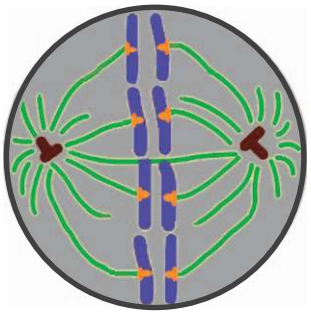


**Figure 9. Illustration showing overrepresented GO "cellular component" categories for SWI/SNF co-purifying proteins.** Overrepresented GO "cellular component" categories are displayed for proteins we detected by IP-mass spectrometry. Centrosomal proteins are shaded brown, chromosomal proteins are blue, kinetochore proteins are orange and cytoskeletal proteins are green. Genes encoding starred proteins are targets of SWI/SNF as identified by ChIP-Seq. Based on these annotations SWI/SNF is associated with multiple cellular components.
doi:10.1371/journal.pgen.1002008.g009

## Materials and Methods

### Chromatin immunoprecipitations

Suspension HeLa S3 cells were cultured by the National Cell Culture Center (Biovest International Inc., Minneapolis, MN) in modified minimal essential medium (MEM), supplemented with 10% FBS at 37°C in 5% $CO_2$, to a density of $6\times10^5$ cells/mL. Cells were fixed with 1% formaldehyde at room temperature for 10 min. Fixation was terminated with 125 mM glycine (2 M stock made in 1x PBS). Formaldehyde-fixed cells were washed in cold Dulbecco's PBS (Invitrogen) and swelled on ice in a 10-mL hypotonic lysis buffer [20 mM Hepes (pH 7.9), 10 mM KCl, 1 mM EDTA (pH 8.0), 10% glycerol, 1 mM DTT, 0.5 mM PMSF, and Roche Complete protease inhibitors, Cat#1697498]. To isolate nuclei, whole cell lysates were homogenized with 30 strokes in a 7 mL Dounce homogenizer (Kontes, pestle B). Nuclear pellets were collected by centrifugation and lysed in 10 mL of RIPA buffer per $3\times10^8$ cells [RIPA buffer: 10 mM Tris-Cl (pH 8.0), 140 mM NaCl, 1% Triton X-100, 0.1% SDS, 1% deoxycholic acid, 0.5 mM PMSF, 1 mM DTT, and protease inhibitors]. Chromatin was sheared with an analog Branson 250 Sonifier (power setting 2, 100% duty cycle for 7×30-s intervals) to an average size of less than 500 bp, as verified on a 2% agarose gel. Lysates were clarified by centrifugation at 20,000× g for 15 min at 4°C.

Clarified nuclear lysates from $1\times10^8$ cells were agitated overnight at 4°C with 20 µg of one of the following antibodies: 1) anti-Ini1 (C-20), Santa Cruz Biotechnology, sc-16189; 2) anti-BAF155 (H-76), Santa Cruz Biotechnology, sc-10756; 3) anti-BAF170 (H-116), Santa Cruz Biotechnology, sc-10757; 4) anti-Brg1 (G-7), Santa Cruz Biotechnology, sc-17796; 5) anti-lamin A/C (H-110), Santa Cruz Biotechnology, sc-20681; 6) anti-lamin B antibody, EMD Biosciences, NA12; or 7) normal IgG, Santa Cruz Biotechnology, sc-2025. Antibody incubations were followed by addition of either protein A (Millipore #16-156) or protein G agarose beads (Millipore #16-266). Beads were permitted to bind to protein complexes for 60 min at 4°C. Immunoprecipitates were washed three times in 1x RIPA, once in 1x PBS, and then eluted in 1xTE/1%SDS. Crosslinks were reversed overnight at 65°C. ChIP DNA was purified by incubation with 200 µg/ml RNase A (Qiagen #19101) for 1 h at 37°C, with 200 µg/ml proteinase K (Ambion AM2548) for 2 h at 45°C, phenol:chloroform:isoamyl alcohol extraction, and precipitation with 0.1 volumes of 3 M sodium acetate, 2 volumes of 100% ethanol and 1.5 µL of pellet paint (Novagen #69049-3). ChIP DNA prepared from $1\times10^8$ cells was resuspended in 50 µL of Qiagen Elution Buffer (EB). Three biological replicates were prepared per antibody.

### Construction and sequencing of Illumina libraries

ChIP-Seq libraries were prepared and sequenced as previously described [26,84]. Biological replicates for each factor were converted into separate and distinct libraries. To summarize, ChIP DNA samples were loaded onto Qiagen MinElute PCR columns, eluted with 15 µL of Qiagen buffer EB, size-selected in the 100–350 bp range on 2% agarose E-gels (Invitrogen) and gel-purified using a Qiagen gel extraction kit. DNA was end-repaired and phosphorylated with the End-It kit from Epicentre (Cat# ER0720). The blunt, phosphorylated ends were treated with Klenow fragment (3′ to 5′ exo minus; NEB, Cat# M0212s) and dATP to yield a protruding 3′-'A' base for ligation of Illumina adapters (100 RXN Genomic DNA Sample Prep Oligo Only Kit, Part# FC-102-1003), which have a single 'T' base overhang at the 3′ end. After adapter ligation (LigaFast, Promega Cat# M8221) DNA was PCR-amplified with Illumina genomic DNA primers 1.1 and 2.1 for 15 cycles by using a program of (i) 30 s at 98°C, (ii) 15 cycles of 10 s at 98°C, 30 s at 65°C, 30 s at 72°C, and (iii) a 5 min extension at 72°C. The final libraries were band-isolated from an agarose gel to remove residual primers and adapters.

Library concentrations and $A_{260}/A_{280}$ ratios were determined by UV-Vis spectrometry on a NanoDrop ND-1000 spectrophotometer (Thermo Fisher Scientific). Purified and denatured library DNA was capture on an Illumina flowcell for cluster generation and sequenced on an Illumina Genome Analyzer II following the manufacturer's protocols [85].

## Identification of proteins by mass spectrometry

Immunoprecipations were performed using the same conditions as for ChIP experiments except the HeLa S3 cells were not crosslinked. In addition to the ChIP antibodies described above we also used anti-Brm, Abcam Cat# ab15597 and anti-BAF250a (PSG3), Santa Cruz Biotechnology, sc-32761. Complexes were resolved on BioRad 4–20% precast Tris-HCl gels (Cat#161-1159) such that a single gel was used for each specific antibody and normal IgG immunoprecipitation pair. Gels were silver stained using Pierce SilverSNAP stain for mass spectrometry (Cat#24600) and each lane was excised into 10–12 molecular weight regions. Gel slices were destained, dried in a Savant speed-vac and digested overnight at 42°C with Sigma's Trypsin Profile IGD kit for in-gel digests (Cat# PP0100). Following the overnight incubation the liquid was removed from each gel piece and volume reduced by drying to approximately 10 µL. The individual gel slices were analyzed separately.

## Mass spectrometry

The samples were subjected to nanoflow chromatography using nanoAcquity UPLC system (Waters Inc.) prior to introduction into the mass spectrometer for further analysis. Mass spectrometry was performed on a hybrid ion trap LTQ Orbitrap mass spectrometer (Thermo Fisher Scientific) in positive electrospray ionization (ESI) mode. The spectra was acquired in a data dependent fashion consisting of full mass spectrum scan (300–2000 m/z) followed by MS/MS scan of the 3 most abundant parent ions. For the full scan in the orbitrap the automatic gain control (AGC) was set to $1\times10^6$ and the resolving power for 400 m/z of 30,000. The MS/MS scans were done using the ion trap part of the mass spectrometer at a normalized collision energy of 24 V. Dynamic exclusion time was set to 100 s to avoid loss of MS/MS spectral information due to repeated sampling of the most abundant peaks.

Sequence data from MS/MS spectra was processed using the SEQUEST database search algorithm (Thermo Fisher Scientific). The resulting protein identifications were brought into the Scaffold visualization software (Proteome Software) where the information was further refined resulting in improved protein id conformation. Scaffold search criteria were set at 98% probability and required at least 2 unique peptides per id.

## Determination of enriched regions in SWI/SNF ChIP-Seq data

All ChIP-Seq data sets (Ini1, Brg1, BAF155, BAF170, and Pol II) were scored against a normal IgG control using PeakSeq [26] with default parameters (q-value$<$0.05) to determine an initial set of enriched regions. These lists were then filtered by removing those regions that did not meet all of the following requirements: 1) the q-value from PeakSeq was further restricted to a q-value of$<$0.01; 2) a minimum of 20 sequencing reads per peak from the specific antibody ChIP; 3) an enrichment of 1.5-fold of the specific antibody relative to the normal IgG control; and 4) an excess of at least 10 of the specific antibody reads relative to the normal IgG control reads. Enriched regions satisfying these criteria comprised our initial list of enrichment sites for each factor (Table1 and Tables S11, S12, S13, S14, S15, and S16). Among these data sources, Pol II and the normal IgG control have been published as part of prior studies and are available in GEO (accession numbers GSE14022 and GSE12781, respectively) [26,84]. Data for Ini1, Brg1, BAF155 and BAF170 can be accessed through GEO series GSE24397.

## Generation of a SWI/SNF union list from ChIP-Seq results

After obtaining our initial list of enriched regions for each factor subjected to chromatin immunoprecipitation, we generated a union list of SWI/SNF component targets. Using the method described in Euskirchen et al. [86], we formed the union of Ini1, BAF155, BAF170, and Brg1 enriched regions as identified by ChIP-Seq and merged any unioned regions that were separated by $\leq$100 bp. Each union region was then classified by whether it intersected with one or more of BAF155, BAF170, Ini1, and Brg1. The resulting list consists of 69,658 SWI/SNF union regions (Table S2).

## Determination of the "high-confidence" and "core" SWI/SNF regions from the ChIP-Seq union regions

We compared our ChIP-Seq target lists for the 69,658 SWI/SNF union regions against genomic features at which chromatin remodeling is expected to play a prominent role: RNA polymerase II sites [26], 5′ ends of Ensembl protein-coding genes, CTCF sites [28], and regions predicted to be enhancers in HeLa cells [29]. We also compared individual SWI/SNF component lists against each other. Only those SWI/SNF regions which intersect another SWI/SNF component or which intersect at least one of the above genomic features were retained for the 'high-confidence' union list. For gene promoter regions, we define overlap as a target region with at least 1 shared bp within $\pm$2.5 kb of the annotated transcription start site (TSS). SWI/SNF region intersections were calculated both for all genes in the Ensembl 52 database build using annotations from NCBI36 (human genome build hg18) as well as for a subset of genes that Ensembl identifies as protein-coding. The resulting target list consists of 49,555 'high-confidence' SWI/SNF union regions (Table S3). Union regions containing all three of the BAF155, BAF170, and Ini1 subunits are designated as the 9,760 'core' SWI/SNF regions (Table3).

## Generating co-occurrence tables

To determine the co-occurrences of features of interest we used a similar intersection strategy as was used for determining the high-confidence SWI/SNF regions. For all pairwise comparisons, one of the two data sets was extended by 100 bp on each side of the region and then intersected against the other, non-extended dataset. We required an overlap of at least 1 bp to deem two regions as associated. Using a Perl script, the intersection results for all comparisons were combined to form the co-occurrence table. The same procedure was followed to generate SWI/SNF-centric (Tables S2 and S3), Pol II-centric (Table S5) and Pol III-centric (Table S6) co-occurrence tables.

## Determination of expressed regions

Using the HeLa RNA-Seq data of Morin et al. [37], we subdivided each list by the expression status of the corresponding gene targets. Expressed genes were defined as any Ensembl gene with an associated Ensembl transcript having an adjusted depth of $\geq$1, representing an average coverage of 1x across all bases in the transcript. A total of 9,711 expressed protein-coding genes satisfied these criteria.

## Comparison of expression levels associated with different SWI/SNF sub-complexes

We created a series of lists based upon the combinations of SWI/SNF components that could co-occur using the 49,555 high-

confidence SWI/SNF regions derived from Table S3. Using the RNA-Seq data of Morin et al. [37], we intersected each list against the 5′ ends of transcripts queried by that study and recorded the corresponding adjusted depth for any transcript with a 5′ end within ±2.5 kb of a SWI/SNF region. Morin et al. treats adjusted depth as a measurement of transcription level for the corresponding transcript. For each list, these measurements were used to build a series of violin plots showing the probability distribution of transcription levels associated with different compositions of SWI/SNF subunits. Note that each SWI/SNF region from Table S2 can only be assigned to one list (e.g. a region containing BAF155, BAF170, and Ini1 is not also assigned to the list of regions containing BAF155 and BAF170).

### Pathway analyses of SWI/SNF factors

Overrepresented GO categories [87] and KEGG pathways [88] were determined using DAVID tools [16]. Figures S2 and S3 were drawn using KGML-ED [89].

### ChIP-chip experimental procedures and array scoring

The ENCODE tiling arrays (NimbleGen Systems Inc., Madison, WI) interrogate the regions from the pilot phase of the ENCODE project [90] and tile the non-repetitive forward strand DNA sequence with 50-mer oligonucleotides spaced every 38 bp (overlapping by 12 bp) for a total of approximately 390,000 features. For array hybridizations ChIP DNA samples from $1\times10^8$ cells were labeled according to the manufacturer's protocol by Klenow random priming with Cy5 nonamers (lamin A/C or lamin B ChIP DNA) or Cy3 nonamers (normal IgG ChIP DNA). Biological replicates, defined as ChIP DNA isolations prepared from distinct cell cultures, were each hybridized to separate microarrays. Each lamin data set consists of three biological replicates. ChIP DNA labeling and array hybridizations were conducted by the NimbleGen service facility (Reykjavik, Iceland). Briefly, arrays were hybridized in Maui hybridization stations for 16–18 h at 42°C, and then washed in 42°C 0.2% SDS/0.2x SSC, room temperature 0.2x SSC, and 0.05x SSC. Arrays were scanned on an Axon 4000B scanner.

For each pair of arrays the files (in GFF file format) corresponding to the two channels for ChIP DNA (635 nm) and reference DNA (532 nm), were uploaded to the TileScope pipeline for normalization and scoring [91]. Data were scored with the following TileScope program parameters: quantile normalization of replicates, iterative peak identification, window size = 500, oligo length = 50, pseudomedian threshold = 1.0, p-value threshold = 4.0, peak interval = 1000, and feature length = 1000. Regions called by Tilescope were then filtered and corrected for multiple hypothesis testing by false discovery rate (FDR). To generate our set of background regions for FDR analysis, we randomly shuffle the probe values within each replicate, ensuring that the same probes are swapped for each replicate. This shuffled data set is then used as input to Tilescope and the scores compared against the lamin A/C and the lamin B data sets. The final lists of enriched regions for lamin A/C and lamin B have a final FDR of 0.1. Target coordinates were converted to hg18 using the UCSC 'liftOver' utility (http://genome.ucsc.edu/cgi-bin/hgLiftOver). Lamin A/C and lamin B data are available through GEO series GSE24382 and Tables S17 and S18.

### Comparison of features across the ENCODE regions

To facilitate comparisons between sequencing and array data we retained only those regions that could be queried by both platforms. To this end, we first identified sequences represented on the ENCODE tiling array that possess less than 25% mappability in ChIP-Seq experiments using 30 bp reads. Any enriched regions in the lamin A/C and the lamin B data sets that were entirely contained within these regions of low mappability were removed from our lists, as corresponding signal levels are unlikely to be detected accurately via ChIP-Seq. Mappability was determined using a 30 bp read length and reported in 100 bp windows according to [26]. The end result is a list of lamin A/C and lamin B enriched regions identified by ChIP-chip in areas of the genome that can be queried by ChIP-Seq. Accordingly, regions that are not represented on the ENCODE tiling arrays were also removed from our SWI/SNF ChIP-Seq experiments for this comparison. Because our ChIP-Seq data covers the entire genome, we began by restricting our enriched SWI/SNF regions only to those that occur in the ENCODE pilot regions. We further refined our ChIP-Seq data set by discarding any SWI/SNF regions that occur in a region of the tiling array for which a signal level of 0 was observed via ChIP-chip. Once our SWI/SNF, lamin A/C, and lamin B lists were limited to those regions that could be queried by both platforms, we intersected the remaining lamin regions and the SWI/SNF regions using the same method that generated the all features table for enhancers, Pol II, and other elements, as described above. Similar procedures were followed for intersections with DNA replication origins identified in the ENCODE regions using tiling arrays [55].

### Evaluating enrichment of SWI/SNF components with respect to other genomic features

To determine whether SWI/SNF components, core regions, and union regions are enriched for factors such as enhancers, small RNAs, lamin A/C and B, CTCF sites, Pol II regions, Pol III sites, 5′ ends and DNA replication origins, we used the genome structure correction test (GSC). This test determines the significance of observations where there "exists a complex dependency structure between observations" and was specifically designed for large-scale genomic studies [27]. Given two lists of genomic regions to compare and a list of coordinates defining the overall sample space (i.e. the length of each chromosome), a p-value for the significance of the overlap of the two lists is calculated and we report this value where noted.

### Data deposition

All data produced for this study can be accessed through GEO and accession numbers for individual series are provided in the relevant sections. Alternatively, data from the lamin ChIP-chip experiments and the Ini1, Brg1, BAF155, and BAF170 ChIP-Seq experiments can be accessed through GEO using the SuperSeries accession number GSE24398.

## Supporting Information

**Figure S1** SWI/SNF signals and target regions in the context of interferon receptor genes on chromosome 21. The coordinates shown are in hg18 and all regions were identified in HeLa cells as detailed in Table S1 and Materials and Methods. The vertical axis for each signal track is the count of the number of overlapping DNA fragments at each nucleotide position and is scaled from 0 to 40 for each track. Panel A displays a ~370 kb region on chromosome 21 containing genes encoding cytokine receptors. Panel B displays a ~20 kb region at the edge of a H3K27me3 domain. Panels C and D each display ~6 kb regions around the 5′ ends of expressed genes.
(EPS)

**Figure S2** SWI/SNF ChIP-Seq targets and interacting proteins superimposed on KEGG 'Pathways in Cancer'. The KEGG 'Pathways in Cancer' network was among those pathways overrep-

resented using our 49,555 SWI/SNF high-confidence union regions (Benjamini adjusted p-value$<4.7\times10^{-8}$). SWI/SNF ChIP-Seq targets are highlighted in yellow and SWI/SNF co-purifying proteins detected in our IP-mass spectrometry experiments are highlighted in blue. SWI/SNF co-purifying proteins reported in other studies (Table S10) are highlighted in red. Proteins or genes not detected in any known SWI/SNF studies are gray. Starred annotations were detected in both ChIP-Seq and protein interaction studies.
(EPS)

**Figure S3** SWI/SNF ChIP-Seq targets and interacting proteins superimposed on KEGG 'Cell Cycle'. The KEGG 'Cell Cycle' network was among those pathways overrepresented using the 49,555 SWI/SNF high-confidence union regions (Benjamini adjusted p-value$<3.7\times10^{-8}$). SWI/SNF ChIP-Seq targets are highlighted in yellow and SWI/SNF co-purifying proteins detected in our IP-mass spectrometry experiments are highlighted in blue. SWI/SNF co-purifying proteins reported in other studies (Table S10) are highlighted in red. Starred annotations were detected in both ChIP-Seq and protein interaction studies.
(EPS)

**Table S1** Data sources.
(DOC)

**Table S2** Features associated with the full union list of 69,658 SWI/SNF ChIP-Seq targets.
(TXT)

**Table S3** Features associated with the high-confidence union list of 49,555 SWI/SNF ChIP-Seq targets.
(XLS)

**Table S4** Combinations of features associated with the 49,555 SWI/SNF ChIP-Seq targets from the union list. For each feature, 1 = present and 0 = absent. The order of features is: 1) Ini1 2) Brg1 3) BAF155 4) BAF170 5) RNA Pol II 6) CTCF 7) Enhancers 8) Five-prime ends 9) Five-prime end-expressed 10) Five-prime ends, non-expressed.
(TXT)

**Table S5** Features associated with the 23,320 RNA Polymerase II ChIP-Seq targets.
(XLS)

**Table S6** Features associated with the 478 RNA Polymerase III ChIP-Seq targets.
(XLS)

**Table S7** Number of transcripts associated with SWI/SNF sub-complexes
(XLS)

**Table S8** Complete lists of Ensembl gene IDs and overrepresented pathways associated with the 49,555 SWI/SNF ChIP-Seq union regions.
(XLS)

**Table S9** Complete lists of Ensembl gene IDs, peptides and overrepresented pathways resulting from mass spectrometry of immunoprecipitated proteins.
(XLS)

**Table S10** Data sources and brief description of interactions displayed in Figure7.
(XLS)

**Table S11** Chromosomal coordinates of the 49,458 Ini1 regions.
(XLS)

**Table S12** Chromosomal coordinates of the 46,412 BAF155 regions.
(XLS)

**Table S13** Chromosomal coordinates of the 30,136 BAF170 regions.
(XLS)

**Table S14** Chromosomal coordinates of the 12,725 Brg1 regions.
(XLS)

**Table S15** Chromosomal coordinates of the 49,555 SWI/SNF union regions.
(XLS)

**Table S16** Chromosomal coordinates of the 23,320 RNA Polymerase II regions.
(XLS)

**Table S17** Chromosomal coordinates of the 1,770 lamin A/C regions.
(XLS)

**Table S18** Chromosomal coordinates of the 1,270 lamin B regions.
(XLS)

**Table S19** Genes encoding SWI/SNF subunits and the chromosomal coordinates of any of the 49,555 SWI/SNF ChIP-Seq union regions that occur in these genes.
(XLS)

## Acknowledgments

We thank Vincent Bruno and Alex Urban for critical reading of the manuscript. Additionally, we thank Nick Carriero and Rob Bjornson for high-performance computing assistance.

## Author Contributions

Conceived and designed the experiments: GME RKA MS. Performed the experiments: GME ED. Analyzed the data: GME RKA ED TAG. Contributed reagents/materials/analysis tools: GME RKA ED TAG GZ JR NB MBG MS. Wrote the paper: GME RKA MS.

## References

1. Jackson DA, Iborra FJ, Manders EM, Cook PR (1998) Numbers and organization of RNA polymerases, nascent transcripts, and transcription units in HeLa nuclei. Mol Biol Cell 9: 1523–1536.
2. Cook PR (1999) The organization of replication and transcription. Science 284: 1790–1795.
3. Cook PR (2010) A model for all genomes: the role of transcription factories. J Mol Biol 395: 1–10. doi:10.1016/j.jmb.2009.10.031.
4. Clapier CR, Cairns BR (2009) The biology of chromatin remodeling complexes. Annu Rev Biochem 78: 273–304. doi:10.1146/annurev.biochem.77.062706.153223.
5. de la Serna IL, Ohkawa Y, Imbalzano AN (2006) Chromatin remodelling in mammalian differentiation: lessons from ATP-dependent remodellers. Nat Rev Genet 7: 461–473. doi:10.1038/nrg1882.
6. Wu JI, Lessard J, Crabtree GR (2009) Understanding the words of chromatin regulation. Cell 136: 200–206. doi:10.1016/j.cell.2009.01.009.

7. Phelan ML, Sif S, Narlikar GJ, Kingston RE (1999) Reconstitution of a core chromatin remodeling complex from SWI/SNF subunits. Mol Cell 3: 247–253.
8. Chen J, Archer TK (2005) Regulating SWI/SNF subunit levels via protein-protein interactions and proteasomal degradation: BAF155 and BAF170 limit expression of BAF57. Mol Cell Biol 25: 9016–9027. doi:10.1128/MCB.25.20.9016-9027.2005.
9. Sohn DH, Lee KY, Lee C, Oh J, Chung H, et al. (2007) SRG3 interacts directly with the major components of the SWI/SNF chromatin remodeling complex and protects them from proteasomal degradation. J Biol Chem 282: 10614–10624. doi:10.1074/jbc.M610563200.
10. Percipalle P, Visa N (2006) Molecular functions of nuclear actin in transcription. J Cell Biol 172: 967–971. doi:10.1083/jcb.200512083.
11. Castano E, Philimonenko VV, Kahle M, Fukalová J, Kalendová A, et al. (2010) Actin complexes in the cell nucleus: new stones in an old field. Histochem Cell Biol 133: 607–626. doi:10.1007/s00418-010-0701-2.
12. Rando OJ, Zhao K, Janmey P, Crabtree GR (2002) Phosphatidylinositol-dependent actin filament binding by the SWI/SNF-like BAF chromatin remodeling complex. Proc Natl Acad Sci U.S.A 99: 2824–2829. doi:10.1073/pnas.032662899.
13. Versteege I, Sévenet N, Lange J, Rousseau-Merck MF, Ambros P, et al. (1998) Truncating mutations of hSNF5/INI1 in aggressive paediatric cancer. Nature 394: 203–206. doi:10.1038/28212.
14. Sévenet N, Lellouch-Tubiana A, Schofield D, Hoang-Xuan K, Gessler M, et al. (1999) Spectrum of hSNF5/INI1 somatic mutations in human cancer and genotype-phenotype correlations. Hum Mol Genet 8: 2359–2368.
15. Wong J, Nakajima Y, Westermann S, Shang C, Kang J, et al. (2007) A protein interaction map of the mitotic spindle. Mol Biol Cell 18: 3800–3809. doi:10.1091/mbc.E07-06-0536.
16. Huang DW, Sherman BT, Lempicki RA (2009) Systematic and integrative analysis of large gene lists using DAVID bioinformatics resources. Nat Protoc 4: 44–57. doi:10.1038/nprot.2008.211.
17. Wiegand K, Shah S, Al-Agha O, Zhao Y, Tse K (2010) ARID1A mutations in endometriosis-associated ovarian carcinomas. N Engl J Med.
18. Jones S, Wang T, Shih I, Mao T, Nakayama K, et al. (2010) Frequent mutations of chromatin remodeling gene ARID1A in ovarian clear cell carcinoma. Science 330: 228–231. doi:10.1126/science.1196333.
19. Van Maele B, Busschots K, Vandekerckhove L, Christ F, Debyser Z (2006) Cellular co-factors of HIV-1 integration. Trends Biochem Sci 31: 98–105. doi:10.1016/j.tibs.2005.12.002.
20. Turelli P, Doucas V, Craig E, Mangeat B, Klages N, et al. (2001) Cytoplasmic recruitment of INI1 and PML on incoming HIV preintegration complexes: interference with early steps of viral replication. Mol Cell 7: 1245–1254.
21. Das S, Cano J, Kalpana GV (2009) Multimerization and DNA binding properties of INI1/hSNF5 and its functional significance. J Biol Chem 284: 19903–19914. doi:10.1074/jbc.M808141200.
22. Isakoff MS, Sansam CG, Tamayo P, Subramanian A, Evans JA, et al. (2005) Inactivation of the Snf5 tumor suppressor stimulates cell cycle progression and cooperates with p53 loss in oncogenic transformation. Proc Natl Acad Sci U.S.A 102: 17745–17750. doi:10.1073/pnas.0509014102.
23. Lee YS, Sohn DH, Han D, Lee H, Seong RH, et al. (2007) Chromatin remodeling complex interacts with ADD1/SREBP1c to mediate insulin-dependent regulation of gene expression. Mol Cell Biol 27: 438–452. doi:10.1128/MCB.00490-06.
24. Xi Q, He W, Zhang XH, Le H, Massagué J (2008) Genome-wide impact of the BRG1 SWI/SNF chromatin remodeler on the transforming growth factor beta transcriptional program. J Biol Chem 283: 1146–1155. doi:10.1074/jbc.M707479200.
25. Simone C (2006) SWI/SNF: the crossroads where extracellular signaling pathways meet chromatin. J Cell Physiol 207: 309–314. doi:10.1002/jcp.20514.
26. Rozowsky J, Euskirchen G, Auerbach RK, Zhang ZD, Gibson T, et al. (2009) PeakSeq enables systematic scoring of ChIP-seq experiments relative to controls. Nat Biotechnol 27: 66–75. doi:10.1038/nbt.1518.
27. Bickel P, Boley N, Brown J, Huang H, Zhang N (2010) Subsampling methods for genomic inference. Annals of Applied Statistics 4: 1660–1697. doi:10.1214/10-AOAS363.
28. Cuddapah S, Jothi R, Schones DE, Roh T, Cui K, et al. (2009) Global analysis of the insulator binding protein CTCF in chromatin barrier regions reveals demarcation of active and repressive domains. Genome Res 19: 24–32. doi:10.1101/gr.082800.108.
29. Heintzman ND, Hon GC, Hawkins RD, Kheradpour P, Stark A, et al. (2009) Histone modifications at human enhancers reflect global cell-type-specific gene expression. Nature 459: 108–112. doi:10.1038/nature07829.
30. Ni Z, Abou El Hassan M, Xu Z, Yu T, Bremner R (2008) The chromatin-remodeling enzyme BRG1 coordinates CIITA induction through many interdependent distal enhancers. Nat Immunol 9: 785–793. doi:10.1038/ni.1619.
31. Bazett-Jones DP, Côté J, Landel CC, Peterson CL, Workman JL (1999) The SWI/SNF complex creates loop domains in DNA and polynucleosome arrays and can disrupt DNA-histone contacts within these domains. Mol Cell Biol 19: 1470–1478.
32. Noma K, Cam HP, Maraia RJ, Grewal SIS (2006) A role for TFIIIC transcription factor complex in genome organization. Cell 125: 859–872. doi:10.1016/j.cell.2006.04.028.
33. Raab JR, Kamakaka RT (2010) Insulators and promoters: closer than we think. Nat Rev Genet 11: 439–446. doi:10.1038/nrg2765.
34. Oler AJ, Alla RK, Roberts DN, Wong A, Hollenhorst PC, et al. (2010) Human RNA polymerase III transcriptomes and relationships to Pol II promoter chromatin and enhancer-binding factors. Nat Struct Mol Biol 17: 620–628. doi:10.1038/nsmb.1801.
35. Barski A, Chepelev I, Liko D, Cuddapah S, Fleming AB, et al. (2010) Pol II and its associated epigenetic marks are present at Pol III-transcribed noncoding RNA genes. Nat Struct Mol Biol 17: 629–634. doi:10.1038/nsmb.1806.
36. Urnov FD, Wolffe AP (2001) Chromatin remodeling and transcriptional activation: the cast (in order of appearance). Oncogene 20: 2991–3006. doi:10.1038/sj.onc.1204323.
37. Morin R, Bainbridge M, Fejes A, Hirst M, Krzywinski M, et al. (2008) Profiling the HeLa S3 transcriptome using randomly primed cDNA and massively parallel short-read sequencing. BioTechniques 45: 81–94. doi:10.2144/000112900.
38. Saunders A, Core LJ, Lis JT (2006) Breaking barriers to transcription elongation. Nat Rev Mol Cell Biol 7: 557–567. doi:10.1038/nrm1981.
39. Fuda NJ, Ardehali MB, Lis JT (2009) Defining mechanisms that regulate RNA polymerase II transcription in vivo. Nature 461: 186–192. doi:10.1038/nature08449.
40. Affymetrix and Cold Spring Harbor Laboratory ENCODE Transcriptome Projects (2009) Post-transcriptional processing generates a diversity of 5'-modified long and short RNAs. Nature 457: 1028–32. doi:10.1038/nature07759.
41. Hanahan D, Weinberg RA (2000) The hallmarks of cancer. Cell 100: 57–70.
42. Malovannaya A, Li Y, Bulynko Y, Jung SY, Wang Y, et al. (2010) Streamlined analysis schema for high-throughput identification of endogenous protein complexes. Proc Natl Acad Sci U.S.A 107: 2431–2436. doi:10.1073/pnas.0912599106.
43. Xue Y, Canman JC, Lee CS, Nie Z, Yang D, et al. (2000) The human SWI/SNF-B chromatin-remodeling complex is related to yeast rsc and localizes at kinetochores of mitotic chromosomes. Proc Natl Acad Sci U.S.A 97: 13015–13020. doi:10.1073/pnas.240208597.
44. Bourgo RJ, Siddiqui H, Fox S, Solomon D, Sansam CG, et al. (2009) SWI/SNF deficiency results in aberrant chromatin organization, mitotic failure, and diminished proliferative capacity. Mol Biol Cell 20: 3192–3199. doi:10.1091/mbc.E08-12-1224.
45. UniProt Consortium (2010) The Universal Protein Resource (UniProt) in 2010. Nucleic Acids Res 38: D142–148. doi:10.1093/nar/gkp846.
46. Misteli T (2007) Beyond the sequence: cellular organization of genome function. Cell 128: 787–800. doi:10.1016/j.cell.2007.01.028.
47. Dechat T, Pfleghaar K, Sengupta K, Shimi T, Shumaker DK, et al. (2008) Nuclear lamins: major factors in the structural organization and function of the nucleus and chromatin. Genes Dev 22: 832–853. doi:10.1101/gad.1652708.
48. Crisp M, Liu Q, Roux K, Rattner JB, Shanahan C, et al. (2006) Coupling of the nucleus and cytoplasm: role of the LINC complex. J Cell Biol 172: 41–53. doi:10.1083/jcb.200509124.
49. Haque F, Lloyd DJ, Smallwood DT, Dent CL, Shanahan CM, et al. (2006) SUN1 interacts with nuclear lamin A and cytoplasmic nesprins to provide a physical connection between the nuclear lamina and the cytoskeleton. Mol Cell Biol 26: 3738–3751. doi:10.1128/MCB.26.10.3738-3751.2006.
50. Shimi T, Pfleghaar K, Kojima S, Pack C, Solovei I, et al. (2008) The A- and B-type nuclear lamin networks: microdomains involved in chromatin organization and transcription. Genes Dev 22: 3409–3421. doi:10.1101/gad.1735208.
51. Reyes JC, Muchardt C, Yaniv M (1997) Components of the human SWI/SNF complex are enriched in active chromatin and are associated with the nuclear matrix. J Cell Biol 137: 263–274.
52. Moir RD, Montag-Lowy M, Goldman RD (1994) Dynamic properties of nuclear lamins: lamin B is associated with sites of DNA replication. J Cell Biol 125: 1201–1212.
53. Cohen SM, Chastain PD, Rosson GB, Groh BS, Weissman BE, et al. (2010) BRG1 co-localizes with DNA replication factors and is required for efficient replication fork progression. Nucleic Acids Res 38: 6906–6919. doi:10.1093/nar/gkq559.
54. Seo S, Herr A, Lim J, Richardson GA, Richardson H, et al. (2005) Geminin regulates neuronal differentiation by antagonizing Brg1 activity. Genes Dev 19: 1723–1734. doi:10.1101/gad.1319105.
55. Cadoret J, Meisch F, Hassan-Zadeh V, Luyten I, Guillet C, et al. (2008) Genome-wide studies highlight indirect links between human replication origins and gene regulation. Proc Natl Acad Sci U.S.A 105: 15837–15842. doi:10.1073/pnas.0805208105.
56. Ryme J, Asp P, Böhm S, Cavellán E, Farrants AO (2009) Variations in the composition of mammalian SWI/SNF chromatin remodelling complexes. J Cell Biochem 108: 565–576. doi:10.1002/jcb.22288.
57. Dinant C, Luijsterburg MS, Höfer T, von Bornstaedt G, Vermeulen W, et al. (2009) Assembly of multiprotein complexes that control genome function. J Cell Biol 185: 21–26. doi:10.1083/jcb.200811080.
58. Rino J, Carvalho T, Braga J, Desterro JMP, Lührmann R, et al. (2007) A stochastic view of spliceosome assembly and recycling in the nucleus. PLoS Comput Biol 3: 2019–2031. doi:10.1371/journal.pcbi.0030201.
59. Luijsterburg MS, von Bornstaedt G, Gourdin AM, Politi AZ, Moné MJ, et al. (2010) Stochastic and reversible assembly of a multiprotein DNA repair complex

ensures accurate target site recognition and efficient repair. J Cell Biol 189: 445–463. doi:10.1083/jcb.200909175.
60. Liu H, Kang H, Liu R, Chen X, Zhao K (2002) Maximal induction of a subset of interferon target genes requires the chromatin-remodeling activity of the BAF complex. Mol Cell Biol 22: 6471–6479.
61. Bouwmeester T, Bauch A, Ruffner H, Angrand P, Bergamini G, et al. (2004) A physical and functional map of the human TNF-alpha/NF-kappa B signal transduction pathway. Nat Cell Biol 6: 97–105. doi:10.1038/ncb1086.
62. Hsiao P, Fryer CJ, Trotter KW, Wang W, Archer TK (2003) BAF60a mediates critical interactions between nuclear receptors and the BRG1 chromatin-remodeling complex for transactivation. Mol Cell Biol 23: 6210–6220.
63. Belandia B, Orford RL, Hurst HC, Parker MG (2002) Targeting of SWI/SNF chromatin remodelling complexes to estrogen-responsive genes. EMBOJ 21: 4094–4103.
64. Weissman B, Knudsen KE (2009) Hijacking the chromatin remodeling machinery: impact of SWI/SNF perturbations in cancer. Cancer Res 69: 8223–8230. doi:10.1158/0008-5472.CAN-09-2166.
65. Barlow CA, Laishram RS, Anderson RA (2010) Nuclear phosphoinositides: a signaling enigma wrapped in a compartmental conundrum. Trends Cell Biol 20: 25–35. doi:10.1016/j.tcb.2009.09.009.
66. Ray A, Mir SN, Wani G, Zhao Q, Battu A, et al. (2009) Human SNF5/INI1, a component of the human SWI/SNF chromatin remodeling complex, promotes nucleotide excision repair by influencing ATM recruitment and downstream H2AX phosphorylation. Mol Cell Biol 29: 6206–6219. doi:10.1128/MCB.00503-09.
67. Ho L, Ronan JL, Wu J, Staahl BT, Chen L, et al. (2009) An embryonic stem cell chromatin remodeling complex, esBAF, is essential for embryonic stem cell self-renewal and pluripotency. Proc Natl Acad Sci U.S.A 106: 5181–5186. doi:10.1073/pnas.0812889106.
68. Ewing RM, Chu P, Elisma F, Li H, Taylor P, et al. (2007) Large-scale mapping of human protein-protein interactions by mass spectrometry. Mol Syst Biol 3: 89. doi:10.1038/msb4100134.
69. Lambert J, Mitchell L, Rudner A, Baetz K, Figeys D (2009) A novel proteomics approach for the discovery of chromatin-associated protein networks. Mol Cell Proteomics 8: 870–882. doi:10.1074/mcp.M800447-MCP200.
70. Gavin A, Bösche M, Krause R, Grandi P, Marzioch M, et al. (2002) Functional organization of the yeast proteome by systematic analysis of protein complexes. Nature 415: 141–147. doi:10.1038/415141a.
71. Gavin A, Aloy P, Grandi P, Krause R, Boesche M, et al. (2006) Proteome survey reveals modularity of the yeast cell machinery. Nature 440: 631–636. doi:10.1038/nature04532.
72. Breitkreutz A, Choi H, Sharom JR, Boucher L, Neduva V, et al. (2010) A global protein kinase and phosphatase interaction network in yeast. Science 328: 1043–1046. doi:10.1126/science.1176495.
73. Lallemand-Breitenbach V, de Thé H (2010) PML nuclear bodies. Cold Spring Harb Perspect Biol 2: a000661. doi:10.1101/cshperspect.a000661.
74. Reyes JC, Muchardt C, Yaniv M (1997) Components of the human SWI/SNF complex are enriched in active chromatin and are associated with the nuclear matrix. J Cell Biol 137: 263–274.
75. Muchardt C, Reyes JC, Bourachot B, Leguoy E, Yaniv M (1996) The hbrm and BRG-1 proteins, components of the human SNF/SWI complex, are phosphorylated and excluded from the condensed chromosomes during mitosis. EMBOJ 15: 3394–3402.
76. Güttinger S, Laurell E, Kutay U (2009) Orchestrating nuclear envelope disassembly and reassembly during mitosis. Nat Rev Mol Cell Biol 10: 178–191. doi:10.1038/nrm2641.
77. Nielsen AL, Sanchez C, Ichinose H, Cerviño M, Lerouge T, et al. (2002) Selective interaction between the chromatin-remodeling factor BRG1 and the heterochromatin-associated protein HP1alpha. EMBOJ 21: 5797–5806.
78. Lavigne M, Eskeland R, Azebi S, Saint-André V, Jang SM, et al. (2009) Interaction of HP1 and Brg1/Brm with the globular domain of histone H3 is required for HP1-mediated repression. PLoS Genet 5: e1000769. doi:10.1371/journal.pgen.1000769.
79. Wilson BG, Wang X, Shen X, McKenna ES, Lemieux ME, et al. (2010) Epigenetic antagonism between polycomb and SWI/SNF complexes during oncogenic transformation. Cancer Cell 18: 316–328. doi:10.1016/j.ccr.2010.09.006.
80. Schuettengruber B, Chourrout D, Vervoort M, Leblanc B, Cavalli G (2007) Genome regulation by polycomb and trithorax proteins. Cell 128: 735–45. doi:10.1016/j.cell.2007.02.009.
81. Kwon SH, Workman JL (2008) The heterochromatin protein 1 (HP1) family: put away a bias toward HP1. Mol Cells 26: 217–227.
82. Ye Q, Callebaut I, Pezhman A, Courvalin JC, Worman HJ (1997) Domain-specific interactions of human HP1-type chromodomain proteins and inner nuclear membrane protein LBR. J Biol Chem 272: 14983–14989.
83. Métivier R, Gallais R, Tiffoche C, Le Péron C, Jurkowska RZ, et al. (2008) Cyclical DNA methylation of a transcriptionally active promoter. Nature 452: 45–50. doi:10.1038/nature06544.
84. Auerbach RK, Euskirchen G, Rozowsky J, Lamarre-Vincent N, Moqtaderi Z, et al. (2009) Mapping accessible chromatin regions using Sono-Seq. Proc Natl Acad Sci U.S.A 106: 14926–14931. doi:10.1073/pnas.0905443106.
85. Bentley DR, Balasubramanian S, Swerdlow HP, Smith GP, Milton J, et al. (2008) Accurate whole human genome sequencing using reversible terminator chemistry. Nature 456: 53–59. doi:10.1038/nature07517.
86. Euskirchen GM, Rozowsky JS, Wei C, Lee WH, Zhang ZD, et al. (2007) Mapping of transcription factor binding regions in mammalian cells by ChIP: comparison of array- and sequencing-based technologies. Genome Res 17: 898–909. doi:10.1101/gr.5583007.
87. Gene Ontology Consortium (2010) The Gene Ontology in 2010: extensions and refinements. Nucleic Acids Res 38: D331–335. doi:10.1093/nar/gkp1018.
88. Kanehisa M, Goto S, Furumichi M, Tanabe M, Hirakawa M (2010) KEGG for representation and analysis of molecular networks involving diseases and drugs. Nucleic Acids Res 38: D355–360. doi:10.1093/nar/gkp896.
89. Klukas C, Schreiber F (2007) Dynamic exploration and editing of KEGG pathway diagrams. Bioinformatics 23: 344–350. doi:10.1093/bioinformatics/btl611.
90. ENCODE Project Consortium (2004) The ENCODE (ENCyclopedia Of DNA Elements) Project. Science 306: 636–640. doi:10.1126/science.1105136.
91. Zhang ZD, Rozowsky J, Lam HYK, Du J, Snyder M, et al. (2007) Tilescope: online analysis pipeline for high-density tiling microarray data. Genome Biol 8: R81. doi:10.1186/gb-2007-8-5-r81.